CHAPTER 2 OVERVIEWS AND THEORY

2.1 Glass Formation

2.1.1. Zachariasen's Rules for the Structure of Glass [60]

In 1932, W.H. Zacharaisen proposed a set of rules that is usually satisfied when an oxide forms a glass. His analysis was based on the following considerations:

(1) The interatomic bonding forces in glasses and crystals must be similar given the similar elastic modulus of the two types of solids.
(2) Like crystals, glasses consist of an extended three dimensional network, but the network does not have translational periodicity.

According to Zachariasen's rules, it has been considered that a substance can form extended three-dimensional networks lacking of periodicity with energy content comparable with that of the corresponding crystal network. These rules were remarkably successful in predicting new glass-forming oxides. The rules are as follows [61]:

(1) An oxygen atom links to not more than two cations.
(2) The number of oxygens surrounding these cations must be small.
(3) The oxygen polyhedra share with one another by their corners, not by their edges or faces.
(4) At least three corners of each polyhedra should be shared.

In a general way, the role of the cations depends on the valence, CN, and the related values of the single-bond strength. Cations of higher valence and lower coordination than the alkalis and alkaline earth oxides may also contribute, in part, to the network structure. So it can be listed the cations in three groups. The different types of ion present in oxide glasses are summarized in Table 2.1.

Table 2.1 Coordination number for glass formers, modifiers and intermediates (adapted from [60]).

Glass formers		Intermediates		Modifiers	
Dopant	CN	Dopant	CN	Dopant	CN
Si	4			Li	1
Ge	4			Na	1
B	3			K	1
Al	3	Al	3	Cs	1
P	5			Rb	1
V	5	Be	2	Be	2
As	5			Mg	2
Sb	5			Ca	2
Zr	4	Zr	4	Ba	2
				Sr	2
		Zn	2	Zn	2
		Cd	2	Cd	2
				Hg	2
				Ga	3
				Sn	4
				Pb	4

(1) Network formers are cations that form coordination polyhedra in glass.
(2) Network modifiers are oxides that do not participate directly in the network.
(3) Intermediate ions can sometimes act in either role.

Oxides, such as SiO_2, B_2O_3, P_2O_5, GeO_2 and BeF_2, are called network formers because of their ability to form branching network structures. These network formers are generally 3 to 4 in coordination numbers. Goldschmidt also considered the crystal structures and their relation to the ionic sizes, and postulated a correlation between the ability to form glass and the relative sizes of the oxygen and cation atoms. The ratios between the radius of cation (R_{cation}) and radius of anion (R_{anion}) in glass-forming oxides are in the range of about 0.2 to 0.4. The radius ratios of typical glass formers are shown in Table 2.2.

Table 2.2 Radius ratios for typical network-formers (adapted from [62]).

Compounds	Radius ratio(R_{cation}/R_{anion})
SiO_2	$R_{Si} : R_{anion}$ = 0.39 Å : 1.4 Å ≈ 0.28
B_2O_3	$R_B : R_{anion}$ = 0.20 Å : 1.4 Å ≈ 0.15
P_2O_5	$R_P : R_{anion}$ = 0.34 Å : 1.4 Å ≈ 0.25
GeO_2	$R_{Ge} : R_{anion}$ = 0.44 Å : 1.4 Å ≈ 0.31
BeF_2	$R_{Be} : R_{anion}$ = 0.34 Å : 1.36 Å ≈ 0.25

2.1.2 Structural Concepts of Glass Formation

A variety of materials form glass readily by cooling from the molten state. It may be recognized that the glass formation range is quite extensive. Many other materials, on the other hand, form a noncrystalline solid only when special techniques, such as cooling from the vapor state, are used. A prime example of this is a - Si: H (amorphous hydrogenated silicon), used extensively for solar cell applications. It is not clear whether most of these amorphous solids are, in fact, glassy solids with a thermodynamic continuity to a supercooled liquid state.

The question of what characteristics make a substance a ready glass former has been the subject of intense research. Historically, the most prevalent thoughts were advanced by Zachariasen. Application of the “random network theory” concepts suggests why oxides such as SiO_2, GeO_2, and B_2O_3, where the oxygen formed tetrahedra or triangles, are ready glass formers, and why compounds such as A_2O and AO have to be ruled out. Figure 2.1 shows a two - dimensional representation of the atomic arrangements in an A_2O_3 glass versus its corresponding crystalline form. (The figure may also correspond to AO_2, where A is tetrahedrally bonded to oxygens, the fourth oxygen being out of the plane of the paper.) Whereas the local oxygen coordination is almost the same as that in a corresponding crystalline solid, the intermediate range order described by ring structures clearly differs considerably between the crystalline and the glassy forms. The glass network consists of holes that are larger than those in the crystal. (The aggregate of the holes yields the free volume discussed above.) When a compound such as Na_2O is introduced in silica, the arrangement of atoms in a two - dimensional plane is believed to look somewhat like that in Figure 2.2 Those oxygens, which connect two silicon tetrahedral at corners, are called bridging oxygens (BOs). Some oxygens are linked to only one silicon; these are called the nonbridging oxygens (NBOs).

Since oxygen is a bivalent ion, its connection to only one silicon ion leaves one negative charge, which is satisfied by a univalent positive sodium ion in the interstitial spaces.

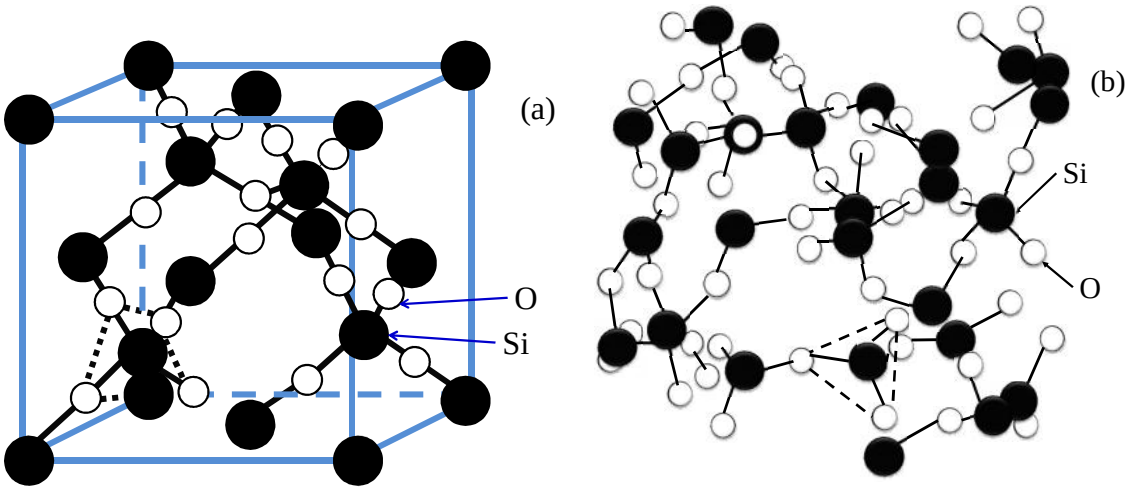

Figure 2.1 A two-dimensional representation of A_2O_3 :
(a) crystal and
(b) glass (adapted from [62]).

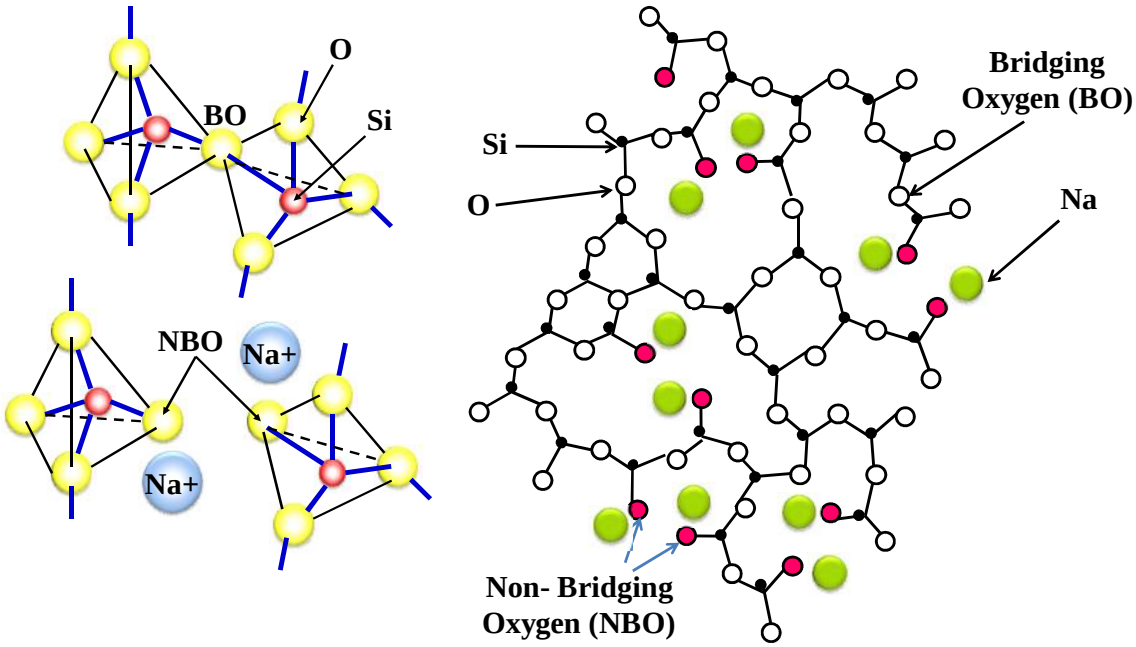

Figure 2.2 A two-dimensional representation of a sodium silicate glass (adapted from [63]).

Much of the early criticism of Zachariasen was based on the discussion of how random is random and, of course, the observation that elements such as S and Se make good glasses yet they did not fit Zachariasen's criteria. Electron microscopy of several otherwise transparent glasses has shown that glass may not be as random as Zachariasen thought and that some type of phase segregation exists in many glasses.

On the basis of the calculation of single bond strengths in an oxide AO_x, Sun suggested that oxides such as B_2O_3, SiO_2, GeO_2, P_2O_5, V_2O_5, and As_2O_5 should be classified as

glass network formers (NWFs), as they ought to be able to form the glass skeleton on their own. Oxides such as Li_2O, Na_2O, K_2O, CaO, BaO, ZnO, CdO, Ga_2O3, In_2O_3, and PbO_2 were classified as glass network modifiers (NWMs); the cations of these oxides occupied the interstitial spaces in the network formed by the NWF oxides and, hence, acted as network modifiers only. Oxides such as BeO, $A1_2O_3$, TiO_2, and ZrO_2 were termed intermediates; these did not make glass readily on their own, but did make a glass when present in large quantities mixed with the NWF or NWM oxides.

B_2O_3 normally functions as a network former in glasses. It is an important composition in special glasses which are used in electro technology, especially in the fields of heat and chemical resistance, excellent electrical insulation, low electrical loss, and gaseous impermeability. B_2O_3 will join the network structure of silica glasses without producing adverse change in the thermal expansion and durability. In the Kovar sealing, the higher percentages of B_2O_3 (17 % - 23 %) are necessary if the glass-transition temperature of glasses must be reduced below 510 $^{\circ}$C**.**

2.2 Structural of B_2O_3 and Borate Glasses [64, 65]

B_2O_3 and borate glasses have been widely investigated, although their technological applications have been mostly in combination with SiO_2. B_2O_3 have the highest glass formation tendency because molten B_2O_3 does not crystallize by itself even when cooled at the slowest rate. B_2O_3 crystallizes only under pressure. Boron is the first member of the Group III in the periodic table. The size of B^{3+} is fit into the trigonal site created by 3 oxide ions in closed contact and forms a $[BO_{3/2}]$ unit. Nevertheless, B - O bond is even more covalent than the Si - O bond. $[BO_{3/2}]$ units are the primary building blocks in all borate glasses. Since B in $[BO_{3/2}]$ is electron deficient (in covalently bonded $[BO_{3/2}]$ unit, B has just 6 electrons in its outermost orbit) it can accept 2 more electrons in the form of a dative bond. This happens when an oxide ion is available in the glass composition for such additional bonding. $[BO_{4/2}]^-$ units are thus readily formed in borate glass structures. $[BO_{4/2}]^-$ units are tetrahedral. From the known covalent radii of B and O, one would expect a B-O bond distance in $[BO_{3/2}]$ unit to be 1.53 Á, which is larger than its experimentally known B - O distance of 1.38 Á. This reduction in the observed distance suggests significant back bonding from the oxygen p - orbitals to the vacant p orbital on B. Several structural studies have been performed on B_2O_3 and it may be fair to say that there is no consensus as to how the building blocks $[BO_{3/2}]$ units are connected in the structure. It is considered that boroxol ring, which consists of 3 $[BO_{3/2}]$ units in hexagonal arrangement of six V - O bonds is a major constituent of glass structure. Boroxol is particularly stable because of the possible delocalization of the electrons among the π bonded p-orbitals of B and O perpendicular to the B - O - B plane as shown in Figure 2.3. On the basis of kinetic studies using XRD, the possible stabilization energy of boroxol unit is found to be 11.8 kcal per boroxol. Glass structure is therefore considered as made up of significant proportions (80 % B atoms or more) of boroxol units which are connected through simple BO_3 units. But the structural models of B_2O_3 glass, in general, fail to account for its observed low density. During modification by added ionic oxides it is suggested that one of the $[BO_{3/2}]$ units in the boroxol structure is transformed into a tetrahedral $[BO_{4/2}]^-$ unit. This destroys the planarity of the boroxol and therefore it shifts the frequency of ring rattling of boroxol from 790 cm^{-1} to 806 cm^{-1} in the Raman spectra.

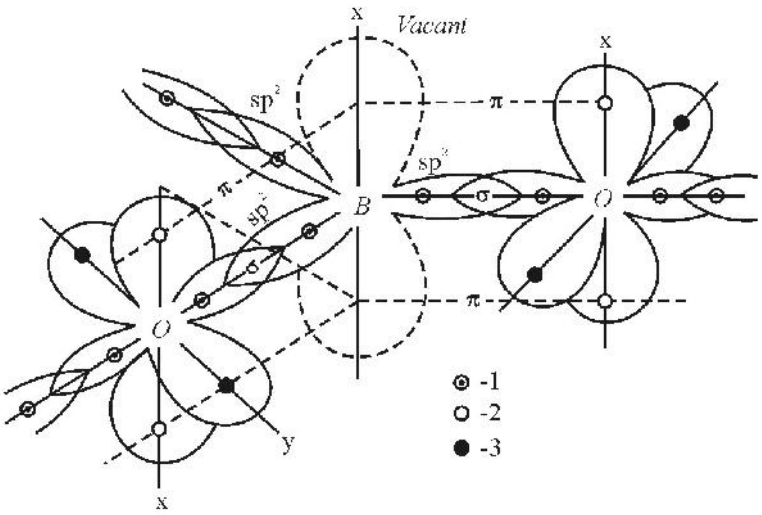

Figure 2.3 The superposition of orbitals in B_2O_3 :
(1) σ-electrons
(2) π-electrons
(3) lone pair electrons (adapted from [65]).

Vibrational spectroscopy has been used with advantage to understand the structure of borate glasses. The classic work of Krogh - Moe in 1965, indicated the possible presence of 5 different types of borate species in the glass structure (Figure 2.4). These are the species which form when B_2O_3 glass is modified by the addition of alkali or alkaline earth oxides [65]. These species are found in the modified B_2O_3 glass with alkali or alkali earth oxide.

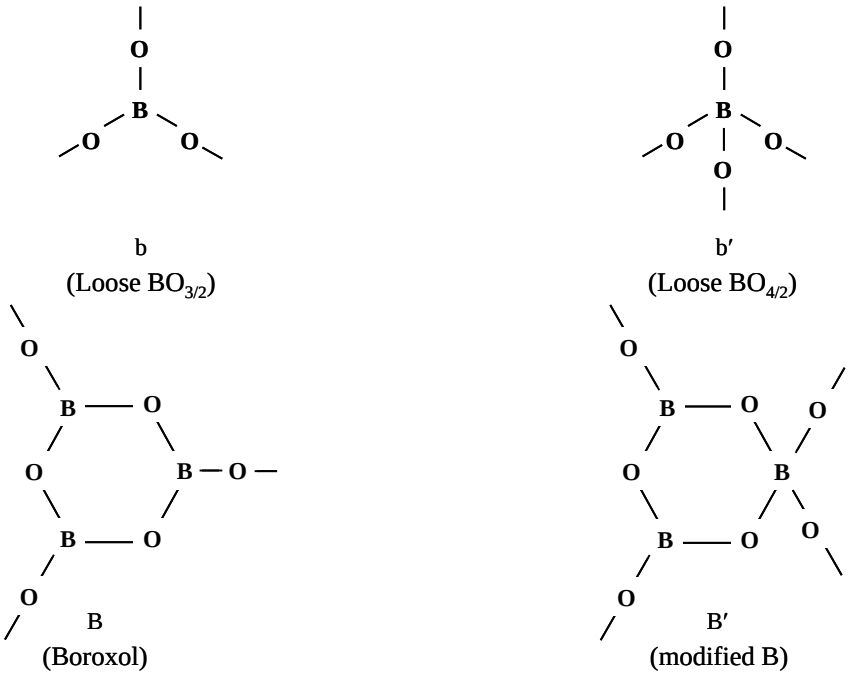

Figure 2.4 Different structural units present in alkali borate glasses (adapted from [65]).

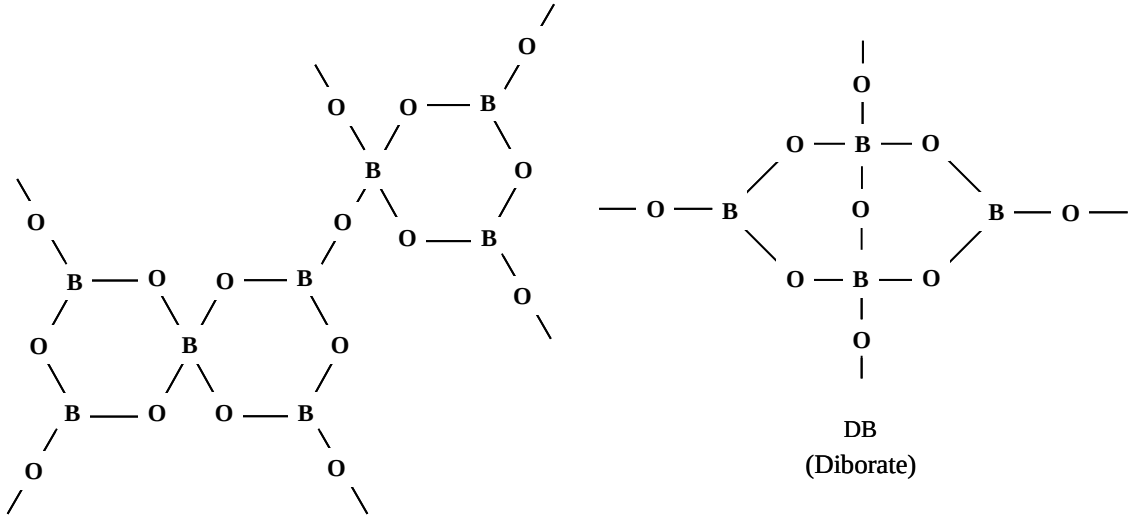

Figure 2.4 Different structural units present in alkali borate glasses (adapted from [65]) continuous.

The boron ion is trivalent positive and is a glass former. The introduction of oxygen from a modifier oxide to boric oxide glass brings about one of the two possibilities [66].

(a) Create a nonbridging oxygen (NBO), as in the silicate glasses, by forming $BO_{2/2}O^-M^+$. (The "$/2$" subscript is denoted for the connection between a bridging oxygen and two borate ion, as shown in Figure 2.5.

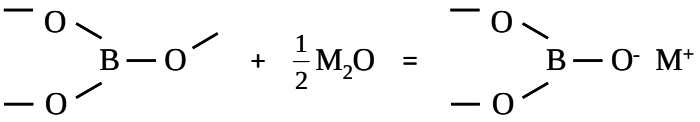

Figure 2.5 Creation of NBO when introduction of modifier to borate glass (adapted from [66]).

(b) Convert boron from a 3 - coordination state ("B_3 state") to a 4 - coodination state ("B_4 state"). Tetrahedral borate, B_4 is commonly found in alkali and alkali earth borate glass. (shown in Figure 2.6)

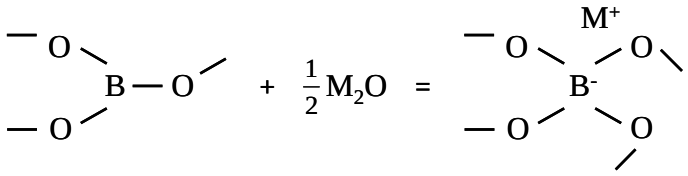

Figure 2.6 Structure change from B3 to B4 introduction of modifier to borate glass (adapted from [66]).

In the BO_3 group, the oxygens are fully bridging, and hence one negative charge from each oxygen satisfies the three positive charges on the boron ion. After the conversion

from B_3 to B_4, all the oxygens remain bridging; the extra negative charge on the $[BO_{4/2}]^-$ group is satisfied by an alkali M^+ ion in the vicinity. The electron transfer from the M atom occurs as a distributed charge density over a large effective diameter BO_4 group, and not localized between the M atom and any specific, oxygen. Since this association is somewhat weak, the alkali ion is expected to become more mobile. However, a coulomb force in the network gives rise the increasing of the network connectivity, and hence flow-related properties (i.e., viscosity increases) and thermal expansion decrease.

In the simplest alkali borate glasses, alkali oxide initially converts the trigonal borons ($[BO_{3/2}]$ units) to tetrahedral borons ($[BO_{4/2}]^-$units) by adding O^{2-} to the trigonal boron unit [65]:

$$2[BO_{3/2}]^0 + O^{2-} \longrightarrow 2[BO_{4/2}]^-$$

$$2B_3 + O^{2-} \longrightarrow 2B_4$$

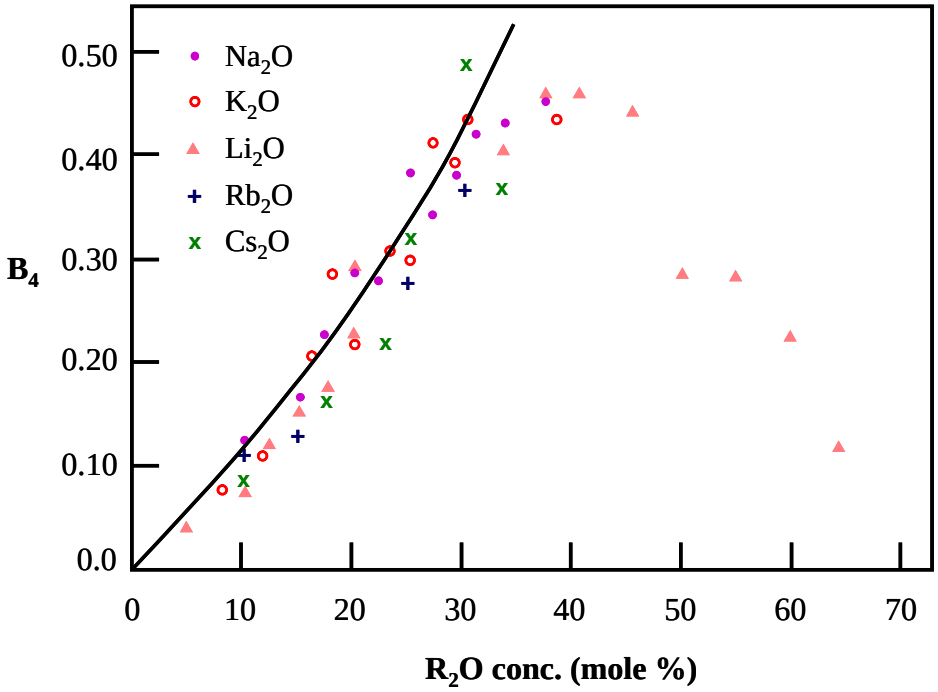

Figure 2.7 Variation of B_4 with R_2O concentration (adapted from [65]).

The formation of B_4 proceeds upon applying an amount of metal oxides until a quantity of B_4 reaches the maximum at 50 % B_4 : 50 % B_3. Interestingly, the quantity of B_4 is decreased when adding the metal oxide more than 50 mole%. (see Figure 2.8). The composition of B_3 and B_4 in diborate glasses is generally equal, and the corresponding mole fraction of the alkali oxide is 0.33. In Figure 2.7, the variation of B_4 (= B_4 / (B_3 + B_4) in various alkali borate glasses) is shown as a function of alkali oxide in mole%. The maximum of B_4 is however, depended on the size of the alkali also. In Figure 2.8 the reason for the rapid decreases in % B_4 upon further adding % R_2O is the reconversion of B_4; i.e. $B_4 \rightarrow B_3$. This has consequences on various observed properties of borate glasses and the effect has been described as “borate anomaly” [67, 69]. The tetrahedral $[BO_{4/2}]^-$ ion is not associated with an NBO, although the unit carries a negative charge. It only means that the negative charge is spread over on all atoms in

the BO_4 unit. Except in the tight structure of diborate units, two B_4 units are not directly connected to borate glasses. In lithium containing glasses, even the diborate glass does not seem to flavor B_4 - B_4 connections. The connectivity of the tetrahedral and the diffuse spread of the negative charge together give rise to an open structure in borate glasses for alkali oxides mole fractions < 0.33. For alkali oxide mole fractions > 0.33, B_4 units breakdown and form $[BO_{1/2}O_2]^{2-}$ units [65]:

$$2[BO_{4/2}]^{-} + O^{2-} \longrightarrow 2[BO_{1/2}O_2]^{2-}$$

$$2B_4 + O^{2-} \longrightarrow 2B_3^{2-}$$

As a consequence, there is a network collapse and better volume utilization. Therefore, rapid reversals occur in the variation of molar volume, refractive indices, glass transition temperature (T_g), thermal expansivity etc., as a function of alkali composition. All of these variations are directly or indirectly related to energy density and are often referred as the borate anomaly. An example of the variation of some of these properties is shown in Figure 2.8.

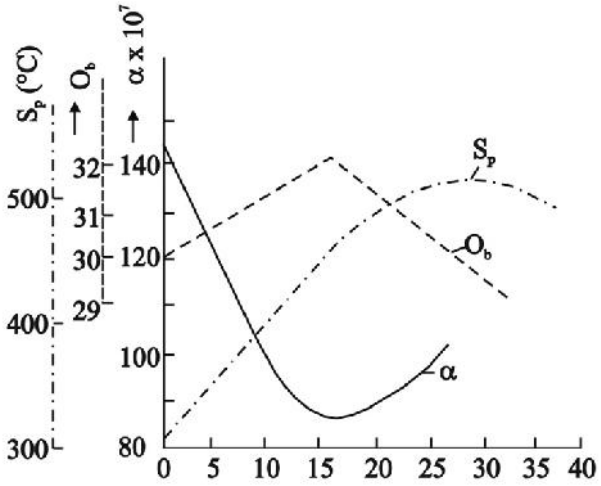

Figure 2.8 Variation in the number of bridging oxygen atoms (O_b), the coefficient of thermal expansion ($\sim_T$) and the softening temperature (S_p) as a function of alkali-oxide concentration in a B_2O_3 containing binary glass (adapted from [65]).

2.3 Molar Volume [68]

The molar volume, symbol V_m is the volume occupied by one mole of a substance (chemical element or chemical compound) at a given temperature and pressure. It is equal to the molar mass (M) divided by the mass density ° . It has the SI unit cubic meters per mole (m^3/mol), although it is more practical to use the units cubic decimeters per mole (dm^3/mol) for gases and cubic centimeters per mole (cm^3/mol) for liquids and solids.

The molar volume of a substance can be found by measuring its mass and density then applying the relation

$$V_m = \frac{M}{\circ}$$

(2.1)

If a sample is mixture containing N components, the molar volume is calculated using:

$$V_m = \frac{\sum_{i=1}^{N} x_i m_i}{\circ_{mixture}} \qquad (2.2)$$

For ideal gases, the molar volume is given by the ideal gas equation : this is a good approximation for many common gases at standard temperature and pressure. For crystalline solids, the molar volume can be measured by X - ray crystallography.

The ideal gas equation can be rearranged to give an expression for the molar volume of an ideal gas:

$$V_m = \frac{V}{n} = \frac{RT}{P} \qquad (2.3)$$

Hence, for a given temperature and pressure, the molar volume is the same for all ideal gases and is known to the same precision as the gas constant : V_m = 8.314 47 $Jmol^{-1}K^{-1}$, that is a relative standard uncertainty of 1.7×10^{-6}. The molar volume of an ideal gas at 100 kPa (1 bar) is 22.710 980(38) dm^3/mol at 0 °C and 24.789 598(42) dm^3/mol at 25 °C.

The molar volume of an ideal gas at 1 atmosphere of pressure is 22.414 L/mol at 0 °C and 24.465 L/mol at 25 °C.

mols are measured $n = \frac{m}{M} = \frac{RT}{P}$; n = mols m = mass M = mass of compound

$$V_m = \frac{N_A V_{cell}}{Z}$$

Crystalline solids

The unit cell volume V_{cell} may be calculated from the unit cell parameters, whose determination is the first step in an X - ray crystallography experiment (the calculation is performed automatically by the structure determination software). This is related to the molar volume by

$$V_m = \frac{N_A V_{cell}}{Z} \tag{2.4}$$

where N_A is the Avogadro constant and z is the number of formula units in the unit cell. The result is normally reported as the crystallographic density.

2.4 Interactions of Gamma and X - Rays with Matter [79-72]

Gamma - rays are electromagnetic radiation, i.e., the release of excess energy from the nucleus of an atom retained after radioactive decay by emission of an alpha particle, but it also emits a gamma-ray at the same time. The gamma-ray emission can be simultaneous or delayed. Similarly, X - rays are electromagnetic radiation that release excess energy from the orbital electrons of an atom. Physically, gamma and X - rays are identical, with the only difference being the point of origin. Gamma-rays are also emitted during fission reactions. Unlike, alpha and beta particles, gamma-rays have no charge or mass; only kinetic energy. Therefore, their method of interaction with materials is markedly different. Instead of having Coulombic interactions with all the electrons in the material around them, gamma-rays only interact intermittently.

Although a large number of possible interaction mechanisms are known for gamma-ray in matter, only the three major types play an important role in radiation physics: the photoelectric effect, Compton scattering, and pair production. All these processes lead to the partial or complete transfer of the gamma - ray photon energy to electron energy. They result in sudden and abrupt changes in gamma - ray photon history, in that photon either disappears entirely or is scattered through a significant angle. When a gamma ray passes near an atom or electron, there is a finite probability that it will interact with that atom or electron or it may not. Gamma - ray can theoretically travel infinite distances without interacting at all.

2.4.1 Compton Scattering or Compton Effect

The interaction process of Compton scattering takes place between the incident photon and a free electron. In the collision, a portion of the gamma - ray's energy is transferred to the electron. Of course, under normal circumstances, all the electrons in a medium are not free but bound. If the energy of the photon, however, is of the order of keV or more, while the binding energy of the electron is of the order of eV, the electron may be considered free. This process is most often the predominant interaction mechanism for gamma-ray energies typical of radioisotope sources.

Figure 2.9 depicts an incoming gamma ray, $E_¥$, colliding with an electron and departing with reduced energy, $E_{¥'}$, and the electron has the remainder of the energy as kinetic energy. The original gamma ray is reduced in energy but continues on until it has

another collision (only its direction of motion and energy change). Therefore, conservation of energy gives (assuming the electron is stationary before the collision) [69]:

$$T_e = E_{¥} - E_{¥'} \tag{2.5}$$

where T_e, $E_{¥}$ *and* $E_{¥'}$ are kinetic energy of the electron, incident photon energy and scattered photon energy, respectively.

If equation (2.5) is used along with the conservation of momentum equations, the energy of the scattered photon as a function of the scattering angle θ can be calculated. The result is [73]:

$$E_{¥'} = \frac{E_{¥}}{1+\left(1-\cos^{-}\right)\frac{E_{¥}}{mc^2}} \tag{2.6}$$

Using equation (2.5) and equation (2.6), one obtains the kinetic energy of the electron.

$$T_e = \frac{\left(1-\cos^{-}\right)\frac{E_{¥}}{mc^2}}{1+\left(1-\cos^{-}\right)\frac{E_{¥}}{mc^2}} E_{¥} \tag{2.7}$$

A matter of great importance for radiation measurement is the maximum and minimum energy of the photon and the electron after the collision. The minimum energy of the scattered photon is obtained when θ = ® this, of course, corresponds to the maximum energy of the electron. From equation (2.6):

$$E_{¥',\min} = \frac{E_{¥}}{1+\frac{2E_{¥}}{mc^2}} \tag{2.8}$$

and

$$T_{e,\max} = \frac{\frac{2E_{¥}}{mc^2}}{1+\frac{2E_{¥}}{mc^2}} E_{¥} \tag{2.9}$$

The maximum energy of the scattered photon is obtained for $\theta = 0$, which essentially means that the collision did not take place. From equation (2.5) :

$$E_{¥',max} = E_{¥} \tag{2.10}$$

$$T_{e,\min} = 0 \tag{2.11}$$

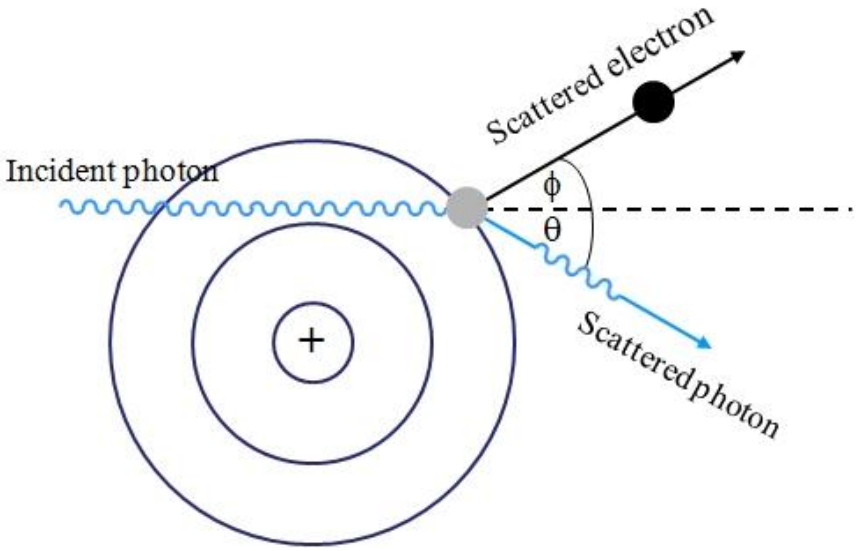

Figure 2.9 The Compton effect (adapted from [69]).

The conclusion to be drawn from equation (2.10) is that the minimum energy of the scattered photon is greater than zero. Therefore, in Compton scattering, it is impossible for all the energy of the incident photon to be given to the electron. The energy given to the electron will be dissipated in the material within a distance equal to the range of the electron. The scattered photon may escape.

The probability that Compton scattering will occur is called the Compton coefficient or the Compton cross section. It is a complicated function of the photon energy, but it may be written in the form [69]:

$$\pm(m^{-1}) = NZf(E_{¥}) \tag{2.12}$$

where ± is the probability for Compton interaction to occur per unit distance, $f(E_{¥})$ is a function of $E_{¥}$. If one writes the atom density N explicitly, equation (2.12) takes the form:

$$\pm \sim \circ \frac{N_A}{A} Zf\left(E_{¥}\right) \sim \circ \left(\frac{N_A}{A}\right)\frac{A}{2} f\left(E_{¥}\right) \sim \circ \frac{N_A}{2} f\left(E_{¥}\right) \tag{2.13}$$

In deriving equation (2.13), use has been made of the fact that for most materials, except hydrogen, $A \approx 2Z$ to $A \approx 2.6Z$. According to equation (2.13), the probability for Compton scattering to occur is almost independent of the atomic number of the material. In Figure 2.10 shows how π changes as a function of $E_{¥}$ and Z. If the Compton cross section is known for one element, it can be calculated for any other by using equation (2.12) (for photons of the same energy):

$$\pm_2\left(m^{-1}\right) = \pm_1\left(\frac{\circ_2}{\circ_1}\right)\left(\frac{A_1}{A_2}\right)\left(\frac{Z_2}{Z_1}\right) \tag{2.14}$$

where $\pm_1$ and $\pm_2$ are given in m^{-1}. If $\pm_1$ and $\pm_2$ are given in m^2/kg, equation (2.14) takes the form:

$$\pm_2\left(m^2/kg\right)=\pm_1\left(\frac{A_1}{A_2}\right)\left(\frac{Z_2}{Z_1}\right) \tag{2.15}$$

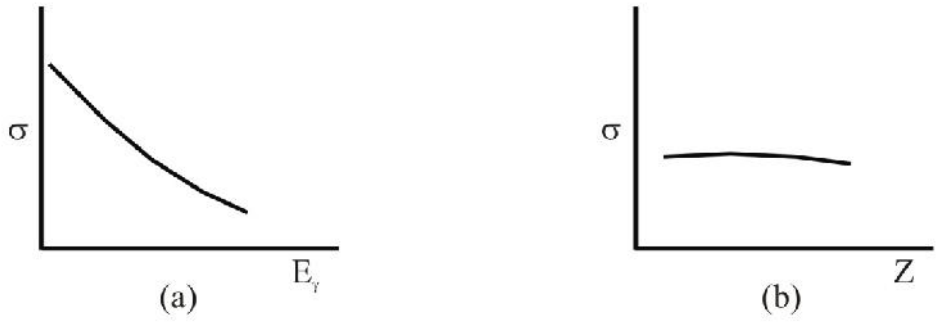

Figure 2.10 Dependence of the Compton cross section on (a) photon energy (b) atomic number of the materials (adapted from [69]).

For Compton effect can be summarized as follows:

- A Compton interaction occurs between a photon and a "free" electron producing a recoiling electron and a scattered photon of reduced energy.
- Kinetic energy transferred to the electron is directly proportional to the scattering angle of the scattered photon and, on average, increases with photon energy.
- The Compton interaction coefficient decreases with increasing energy and is almost independent of atomic number.

2.4.2 Photoelectric Effect

In photoelectric effect, a photon undergoes an interaction with a bound atomic electron and eject it from the atom, occurs when a gamma ray is absorbed by an electron and the kinetic energy of the gamma ray is transferred to the electron. As a result of the interaction, the photon completely disappears and one of the atomic electrons is ejected as a free electron, called the photoelectron. Figure 2.11 depicts an incoming gamma - ray being absorbed by an electron which then shoots off with a kinetic energy equal to the incoming gamma - rays energy minus the binding energy of the electron to the atom. The original gamma ray has been stopped and eliminated and replaced by an photoelectron which its kinetic energy, T_e is

$$T_e = E¥ - B.E. \tag{2.16}$$

where $E¥$ is energy of the incident photon
$B.E.$ is binding energy of electron

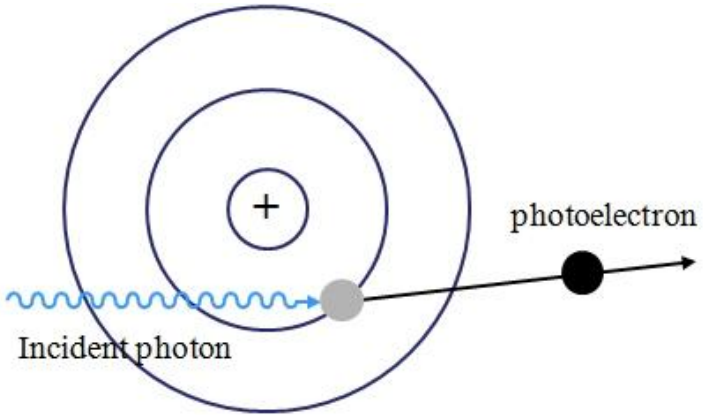

Figure 2.11 The Photoelectric effect (adapted from [69]).

The photoelectric process is the predominant mode of interaction for gamma or X - rays of relatively low energy. The probability of this interaction occurring is called the photoelectric cross - section or photoelectric coefficient, ², increases rapidly with atomic number of the target atom. In addition, it also has a strong. It is a function of the atomic number (*Z*) of the absorbing material (generally related to the density *ρ* of the absorbing medium), gamma rays energy (*E*¥). The equation giving ² may be written as [65]:

$$²\left(m^{-1}\right) = aN\frac{Z^{n}}{E_{¥}^{m}}\left[1 - ¯(Z)\right] \tag{2.17}$$

where ² is probability for photoelectric effect to occur per unit distance traveled by the photon
a is constant, independent of *Z* and *E*¥
m,*n* is constants with a value of 3 to 5 (their value depends on *E*¥)
N is number of atom/m^3

The term in parentheses indicates correction terms of the first order in *Z*. Figure 2.12 shows how the photoelectric coefficient changes as a function of E_γ and *Z*. As Figure 2.12 and equation (2.17) show, the photoelectric effect is more important for high-*Z* material, i.e., more probable in Pb (*Z* = 82) than in Al (*Z* = 13). It is also more important for *E*¥ = 10 keV than *E*¥ = 500 keV (for the same material).

Using equation (2.17), one can obtain estimates of the photoelectric coefficient of one element in terms of that of another. If one takes the ratio of ² for two elements, the result for photons of the same energy is [69]:

$$²_{2}\left(m^{-1}\right) = ²_{1}\frac{°_{2}}{°_{1}}\left(\frac{A_1}{A_2}\right)\left(\frac{Z_2}{Z_1}\right)^{n} \tag{2.18}$$

where *ρ* and *A* represent the density and atomic weight, respectively, of the two elements, and ²*1* and ²*2* are given in m^{-1}. If ²*1* and ²*2* are given in m^2/kg, equation (2.18) takes the form [62]:

$$\text{²}_2\left(m^2/kg\right)=\text{²}_1\frac{A_1}{A_2}\left(\frac{Z_2}{Z_1}\right)^n \tag{2.19}$$

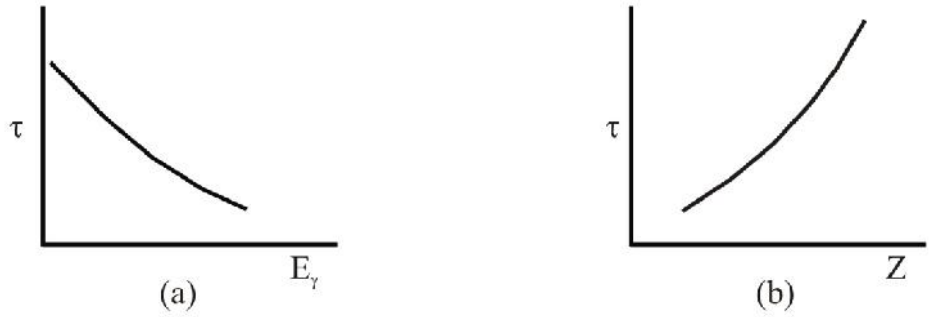

Figure 2.12 Dependence of the photoelectric cross-section on (a) photon energy and (b) atomic number of the material (adapted from [69]).

The photoelectric effect can be summarized as follows:

- It occurs only with bound electrons because the entire atom is necessary to conserve momentum.
- The interaction coefficient is greatest when the photon energy just equals the amount to overcome the binding energy of the orbital electron, causing it to be ejected from its shell.
- The photoelectric absorption coefficient is directly proportional to Z^5 and inversely proportional to $E_¥^3$ on average.

2.4.3 Pair Production

Pair production is an interaction occurs when the photon energy exceeds twice the rast mass energy of an electron (1.02 MeV), the process of pair production is energetically possible. As a result of the interaction, the photon disappears and an electron-positron pair appears (Figure 2.13). Although the nucleus does not undergo any change as a result of this interaction, its presence is necessary for pair production to occur. A gamma-ray will not disappear in empty space by producing an electron-positron pair.

Conservation of energy gives the following equation for the kinetic energy of the electron and the positron:

$$T_{e^-}+T_{e^+}=E_¥-\left(mc^2\right)e^-\left(mc^2\right)e^+=E_¥-1.022\ \text{MeV} \tag{2.20}$$

Pair production may take place in the field of an electron. The probability for that to happen is much smaller and the threshold for the threshold for the gamma energy is $4mc^2$ = 2.04 MeV.

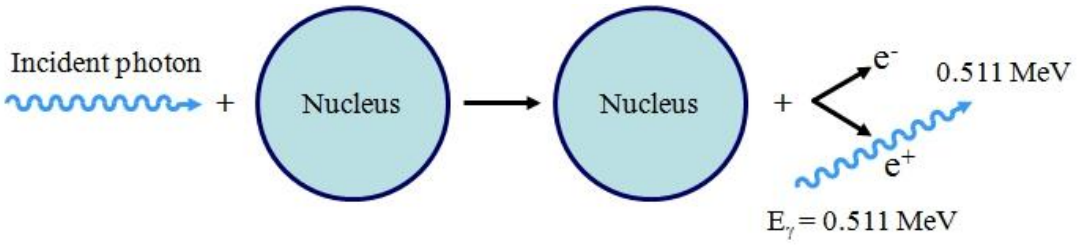

Figure 2.13 Pair production. The gamma disappears and a positron-electron pair is created. Two 0.511 MeV photons are produced when the positron annihilates (adapted from [69]).

The available kinetic energy is equal to the energy of the photon minus 1.022 MeV, which is necessary for the production of the two rest masses. Electron and positron share, for all practical purposes, the available kinetic energy, i.e.:

$$T_{e^-} = T_{e^+} = \frac{1}{2}\left(E_{¥} - 1.022\ \text{MeV}\right) \tag{2.21}$$

Pair production eliminates the original photon, but two photons are created when the positron annihilates. The annihilation gammas are important in constructing shielding against them as well as for the detection of gammas.

The probability for pair production to occur, called the pair production coefficient or cross section, is proportional to the square of the atomic number *Z* for photons with energy greater than 2 x 0.511 MeV. It may be written in the form:

$$©\left(m^{-1}\right) = NZ^2 f\left(E_{¥}, Z\right) \tag{2.22}$$

where © is the probability for pair production to occur per unit distance traveled and *f(E, Z)* is a function, which change slightly with *Z* and increases with $E_{¥}$.
In Figure 2.14 shows how κ changes with $E_{¥}$ and *Z*. It is important to note that © has a threshold at 1.022 MeV and increases with $E_{¥}$ and *Z*. Of the three coefficients (² and ® being the other two), © is the only one increasing with the energy of the photon.

If the pair production cross-section is known for one element, an estimate of its value can be obtained for any other element by using equation (2.22) (for photons of the same energy):

$$©_2\left(m^{-1}\right) = ©_1\left(\frac{°_2}{°_1}\right)\left(\frac{A_1}{A_2}\right)\left(\frac{Z_2}{Z_1}\right)^2 \tag{2.23}$$

where $©_1$ and $©_2$ are given in m^{-1}.

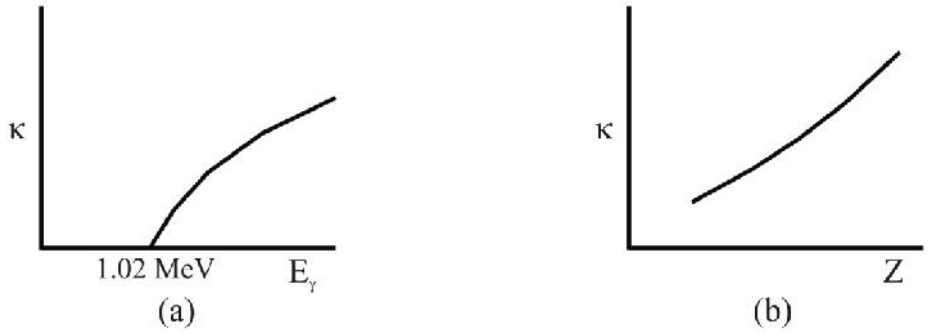

Figure 2.14 Dependence of the pair-production cross section on (a) photon energy and (b) atomic number of the material (adapted from [69]).

Pair production can be summarized as follows:

- They occur for photons with $E_¥ \geq 1.022$ MeV primarily in the field of the nucleus to produce two electron masses with kinetic energy, but can also occur with an orbital electron yielding a triplet of electron masses.
- The kinetic energy shared between the positron and the electron is $E_¥$ - 1.022 MeV.
- The positron annihilates with a free electron after dissipating its kinetic energy to produce two 0.511 MeV annihilation photons.
- The absorption coefficient increases rapidly with energy above the 1.022 MeV threshold and varies approximately as Z^2.

2.5 Gamma - Ray Attenuation Coefficient [69-72]

When a photon penetrates through matter, it may interact through any of the three major interactions discussed earlier. (For pair production, $E_¥ >1.022$ MeV.). There are other interactions, but they are not mentioned here because they are not important in the detection of gamma-rays.

Figure 2.15 shows the relative importance of the three interactions as $E_¥$ and Z change. Consider a photon with $E = 0.1$ MeV, if this particle travels in carbon ($Z = 6$), the Compton effect is the predominant mechanism by which this photon interacts. If the same photon travels in iodine ($Z = 53$), the photoelectric interaction prevails. For a γ of 1MeV, the Compton effect predominates regardless of Z. If a photon of 10 MeV travels in carbon, it will interact mostly through Compton scattering. The same photon moving in iodine will interact, mainly, through pair production.

The total probability for interaction per unit path length μ, called the total linear attenuation coefficient, is equal to the sum of the three probabilities:

$$« = ² \textit{(photoelectric)} + ² \textit{(Compton)} + © \textit{(pair)} \qquad (2.24)$$

where μ is the probability of interaction per unit distance.

There are tables that give μ for all the elements, for many photon energies. Most of the tables provide μ in units of m^2/kg. (or cm^2/g), because in these units the density of the material does not have to be specified.

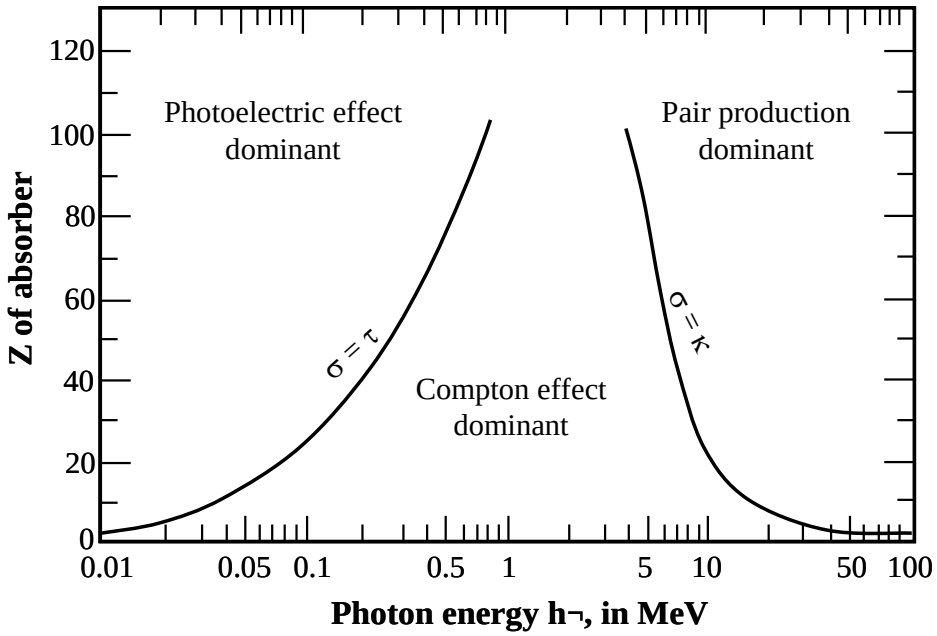

Figure 2.15 The relative importance of the three major gamma interactions (adapted from [72]).

The total linear attenuation coefficient in the above relations determines how quickly or slowly a certain photon beam will attenuate while passing through a material. It is a function not only of the photon energy but also of the type and density of the material. Therefore, the mass attenuation coefficient, $«_m$, is much more widely uses is defined:

$$«_m = \frac{«}{\circ} \tag{2.25}$$

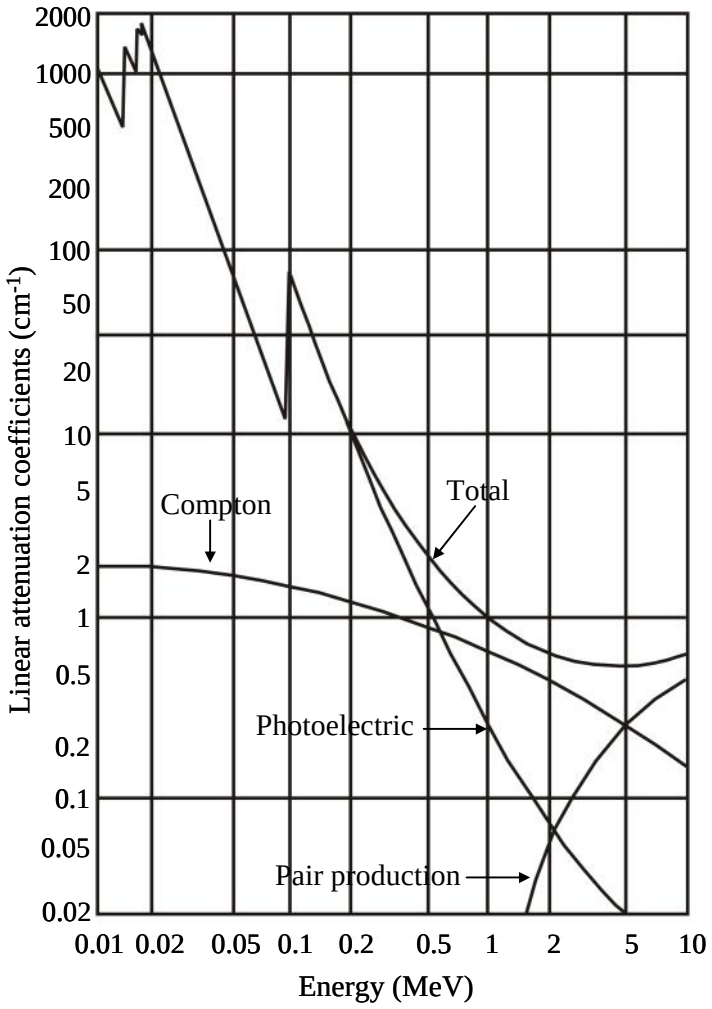

Figure 2.16 Mass attenuation coefficients for lead (Z = 82, ° $= 11.35 \times 10^3$ kg/m^3) (adapted from [72]).

Figure 2.16 shows the individual coefficients as well as the total mass attenuation coefficient for lead, as a function of photon energy. The total mass attenuation coefficient shows a minimum because as E increases, ² decreases, © increases, and σ does not change appreciably. However, the minimum of μ does not fall at the same energy for all elements. For lead, μ is minimized at E¥ ~ 3.5 MeV; for aluminum, the minimum is at 20 MeV; and for NaI, the minimum is at 5 MeV.

2.5.1 Measuring Attenuation Coefficients

If a parallel beam of monoenergetic gamma-rays goes through a material of thickness x, the fraction of the beam that traverses the medium without any interaction is equal to $e^{-\alpha x}$ (see Figure 2.17). The probability that a photon will go through thickness x without an interaction is:

$$I = I_0 e^{-\alpha x} \tag{2.26}$$

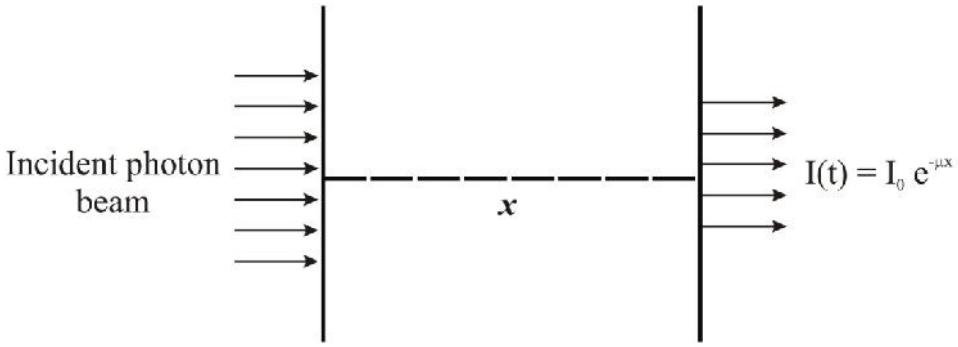

Figure 2.17 The intensity of the transmitted beam (only particles that did not interact) decreases exponentially with material thickness (adapted from [69]).

As particles pass through material, they undergo collisions that may change their direction of motion. The average distance between these collisions is therefore a measure of the probability of a particular interaction. This distance, generally known as the mean free path (*MFP*), that is

$$MFP = \frac{\int_0^\infty x e^{-\mu x} dx}{\int_0^\infty e^{-\mu x} dx} = \frac{1}{\mu} \tag{2.27}$$

Thus, the mean free path is simply the inverse of the total linear attenuation coefficient. If $\mu = 10\ m^{-1}$ for a certain γ-ray traveling in a certain medium, then the distance between two successive interactions of this gamma in that medium is $MFP = 1/\mu = 1/10$ m = 0.10 m.

2.5.2 Mixture and Compounds

The attenuation coefficient of a compound or mixture at a certain energy can be obtained by simply taking the weighted mean of its individual components according to The total mass attenuation coefficient for a compound or a mixture is calculated by: [69, 74]

$$\mu_m = \sum_{i=1}^{n} w_i (\mu_m)_i \tag{2.28}$$

where μ_m is total mass attenuation coefficient for a compound or a mixture
w_i is weight fraction of i^{th} element in the compound
$(\mu_m)_i$ is total mass attenuation coefficient of i^{th} element.

2.6 Effective Atomic Numbers and Effective Electron Density

In this section we summarize theoretical relations used in the present work. A parallel beam of monoenergetic gamma-ray photons is attenuated in matter according to the Lambert-Beer law [69]:

$$I = I_0 \, e^{-\mu_m \rho x} \tag{2.29}$$

where I_0 and I are incident and transmitted intensities of gamma radiation, respectively. μ_m is the mass attenuation coefficient for absorber, x is the thickness of absorber and ρ is the density of absorber.

Theoretical values of the mass attenuation coefficients of mixture or compound have been calculated by Win X Com, based on the mixture rule from equation (2.28).

This mixture rule is valid when the effects of molecular binding, chemical and crystalline environment are negligible. The values of mass attenuation coefficients can be used to determine the total atomic cross-section ($\sigma_{t,a}$) by the following relation [78]:

$$\sigma_{t,a} = \frac{(\mu_m)}{N_A \sum_i^n (w_i / A_i)} \tag{2.30}$$

where N_A is Avogadro's number, A_i is atomic weight of the constituent element of mixture . Also the total electronic cross-section ($\sigma_{t,el}$) for the element is expressed by the following formula [75]:

$$\sigma_{t,el} = \frac{1}{N_A} \sum_i^n \frac{f_i A_i}{Z_i} (\mu_m)_i \tag{2.31}$$

where f_i is the number of atoms of the element i^{th} relative to the total number of atoms of all elements in mixture, Z_i is the atomic number of the i^{th} element in alloy.

Atomic number, Z, is and ubiquitous parameter in atomic and nuclear physics where it occurs in almost any formula. For a complex medium, the effective atomic number, Z_{eff}, is a convenience parameter for representing gamma and X - ray interactions. However, a single number cannot represent the effective atomic number of a material, which s composed of several elements. Accordingly, Z_{eff}, is no true constant for a given material, but a parameter varying with photon energy with photon energy depending on the interaction processes involved. The effective atomic number is closely related to the electron density, express in number of electron per unit mass.

By using the mass attenuation coefficient of mixture, the effective atomic number (Z_{eff}) and the effective electron density (N_e) (number of electrons per unit mass) were determined from equation (2.30) and equation (2.31), respectively [75]:

$$Z_{eff} = \frac{\sigma_{t,a}}{\sigma_{t,el}} \tag{2.32}$$

Finally, the effective number, N_e, of electrons per unit mass of the absorber can be found from

$$N_e = \frac{\mu_m}{\sigma_{t,el}} \tag{2.33}$$

2.7 Optical Properties [76]

There are many advanced and exciting applications of glasses in optics: optical fibers as waveguides for long and fast telecommunications, laser hosts, and optical components for medical and outer space studies. Other modern glass are glasses that change absorption with light level (photochromic) and electric field (electrochromic), glasses for gradient index lenses, the new glasses such as fluorides with different optical properties for silicate planar waveguides, sensors, and chalcogenide glasses with high non-linear optical properties for switching, all optical devices and photonic applications.

For the glass window and the glass bulb to function, the optical transmission property is important. The correction for the failing vision and glass fiber communication are based upon the refractive index, optical dispersion and transmission properties of glass. Beside these, there are many more technological advances where the optical properties of glass play a pivotal role.

The linear refractive index (n), and its dispersive wavelength dependence are important parameters to determine the suitability of oxide glass as optical materials. The propagation of electromagnetic waves depends on the optical constants of materials n and k (the extinction coefficient), where n affects the phase of light waves propagate in the material while k affects its amplitude.

The presence of chemical addition can be altering the refractive index and the transmission range. Glasses are differ considerably in structure and thus in the position and intensity distribution of their electronic absorption and vibrational spectra. Color glass filters are made by adding semiconductors with the band gaps in the visible spectral region during the fusion process.

Visible (VIS) region, light rays are generally referred to by their wavelength λ stated in nanometers or angstroms. Infrared (IR) region, the wave number ($2\pi/\lambda$) with units cm^{-1} is used. Ultraviolet (UV) region, sometimes the energy E (eV units) of the photons is used. For conversion, 1 eV = 1,239.8/λ (nm).

When light travels through a medium, a part of it is reflected from the front surface, a part is absorbed, and the balance is transmitted. The reflectance *R* at normal incidence for light waves traveling from one dielectric medium to another is given by

$$R = \left(\frac{n_1 - n_2}{n_1 + n_2} \right)^2 \tag{2.34}$$

Where, the refractive index or the index of refraction *n* is ratio between the speed of light in vacuum and the speed of light in that medium.

When light waves travel from one medium of refractive index n_1 into another medium of refractive index n_2, the incident and the refracted rays remain in the same plane, an incident angle θ_i and refractive angle θ_r (angles between the ray and the normal line) are related through Snell's law or law of refraction.

$$\frac{\sin\theta_r}{\sin\theta_i} = \frac{n_1}{n_2} \tag{2.35}$$

When $n_1 > n_2$, $r = 90^o$ at the critical angle of incidence ¤c (called Brewster's angle). Upon $i >$ ¤c, the incident ray is total internally reflected. The bending of light rays as they pass from one medium to another is the key to the design of lenses in eyeglasses, microscopes, telescopes, and camera.

The absorption coefficient (α) is defined by Beer-Lambert's law for intensity I transmitted through a distance z of medium:

$$I = I_0 e^{-\tilde{}z} \tag{2.36}$$

where I_0 is the incident intensity.
The absorption as due to a solution of the absorbing species in the medium, in which case it is useful to define a molar extinction coefficient ¢ as

$$a = \delta c \tag{2.37}$$

Where c is the concentration (mol/L) of the absorb center. ¢ is expressed as L/mol/cm. The absorbance (A) and the optical density (D) are given by

$$A = -\ln\left[\frac{I}{I_0}\right] \tag{2.38}$$

$$D = -\log\left[\frac{I}{I_0}\right] \tag{2.39}$$

Other important criterion in the design of optical components to be considered is the correction for chromatic aberration resulting from the dispersion of light, i.e., the variation of n with wavelength. Away from an absorption peak, n may be expressed by Cauchy's dispersion formula:

$$n = A' + \frac{B'}{\lambda^2} + \frac{C'}{\lambda^4} + \ldots, \tag{2.40}$$

where Aà, Bà, Cà,… are known as Cauchy coefficients which are characteristic of the material. These coefficients are defined as

$$A' = 1 + \sum_{j=i+1}^{\infty} a_{ij}\ ,\ B' = 1 + \sum_{j=i+1}^{\infty} a_{ij}\lambda_{ij}^2\ ,\ C' = 1 + \sum_{j=i+1}^{\infty} a_{ij}\lambda_{ij}^4 \tag{2.41}$$

where $a_{ij} = r_e N f_{ij} \lambda_{ij}^2 / 2\pi$, r_e = 2.818x10^{-13} cm is the radius of an excited electron experiencing a transition from a lower energy level i to a higher energy level j when it absorbs a photon associated with a (transition) wavelength λ_{ij}. N is the atomic number

density. The oscillator strength f_{ij} is a fraction of N which takes part in a given $i \rightarrow j$ transition.

For practical purposes, the useful parameters in the correction for chromatic aberration are the Abbe number ¬$_d$ and the partial dispersion. The Abbe number is defined by

$$\nu_d = \frac{n_d - 1}{n_F - n_C} \tag{2.42}$$

where the F-line is the blue λ = 486.1327 nm line from the hydrogen spectrum, the C - line is red λ = 656.2725 nm line, also from the hydrogen spectrum, and the d-line is the yellow λ = 587.5618 nm line from the He spectrum. The partial dispersion for any two wavelengths x and y is given by

$$P_{x,y} = \frac{n_x - n_y}{n_F - n_C} \tag{2.43}$$

In optical applications of glasses, a map of the variation of refractive index as a function of Abbe number (dispersion) is used. In conventional maps, the designations of the glasses are given as “Crown” and “Flint”, which is somewhat confusing. Highly refractive glasses tend to have smaller Abbe numbers, i.e., high relative dispersion. A high refractive index is desirable to increase glass reflectivity (shiny appearance).

The factors affecting refractive - index of the glass are

1. Polarizability of the first neighbor ions coordinated with it (anion).
2. Field intensity Z/a^2 (i.e., polarization power), where Z is the valence of the ion (ionic charge) and a is the distance of separation (ionic radius).
3. Coordination number of the ion.
4. Non-bridging oxygen bonds (NBOs).
5. Electronic polarizability of the oxide ion.
6. Optical basicity of the glasses.

According to Fajan’s rules the first two factors mean that to increase electronic polarizability of the material a small positive ion (cation), a large negative ion (anion), and large charges on either ion are required. In the scope of previous factors, the refractive indices behavior of the different glass samples can be analyzed and explained.

2.8 Absorption Processes in Solids [77]

In describing absorption processes in solids, it is possible to categorize the major phenomena under six headings. They are, in order of commonly encountered decreasing energy of the transition :

(1) Electron transitions from the valence band to higher-lying conduction bands, characterized by continuous high - absorption processes with structure variations depending on the density of states distribution in the bands involved. The optical absorption constant in usually in the range 10^5 - 10^6 cm^{-1}.

(2) Electron transitions form the valence band to the lowest-lying conduction band with a minimum required energy of the forbidden band gap. The magnitude and variation with energy of the absorption constant depends on whether the transition involves a photon only (direct transition) or whether it involves both a photon and a phonon (indirect transition). The absorption constant decreases by many orders of magnitude as the photon energy drops below the band gap energy.

(3) Optical excitation producing a bound electron - hole pair, known as an *exciton*, requiring less energy than to produce a free electron - hole pare by excitation across the band gap. The exciton can be thought of as a hydrogenic system, capable of moving and transporting energy through the crystal without transporting net charge. The electron and hole making up an exciton may be thermally dissociated into free carriers, or may recombine with the emission of light or phonons.

(4) If imperfections are present in the crystal, they create energy levels that lie in the forbidden gap. Therefore at energies less than the band - gap energy it is still possible to excite electrons to the conduction band from imperfection levels occupied by electrons, of to excite electrons from the valence band to unoccupied imperfection levels, each process giving rise to optical absorption. This absorption in turn comes to an end when the photon energy is less than the energy required to make a transition from the imperfection level to one of the bands. For very high imperfection densities, the corresponding absorption constant may have values as high as 10^3 cm^{-1}, but in general is considerably less.

(5) Absorption of photons by free carriers, causing a transition to higher energy states within the same band or to higher bands. This process can occur over a wide range of photon energies. It involves the absorption of both photons and phonons since both energy and *k* must be charged in the transition. There is also an optical absorption due to free carriers action collectively as a kind of “electron gas” which is known as plasma resonance absorption.

(6) Absorption of photons in the excitation of optical mode vibrations of the crystal lattice, known as Reststrahlen absorption. This is the only one of six phenomena that does not involve electronic transitions Figure 2.18 illustrates these various electronic absorption process in both flat - band and *E* vs *k* diagrams. Note that the *E* vs *k* diagrams tell about both changes in *E* and change in *k* during an optical transition, whereas the flat - band diagram can be describe only changes in *E*. In the following section, we consider process 2 - 5 in a little more detail.

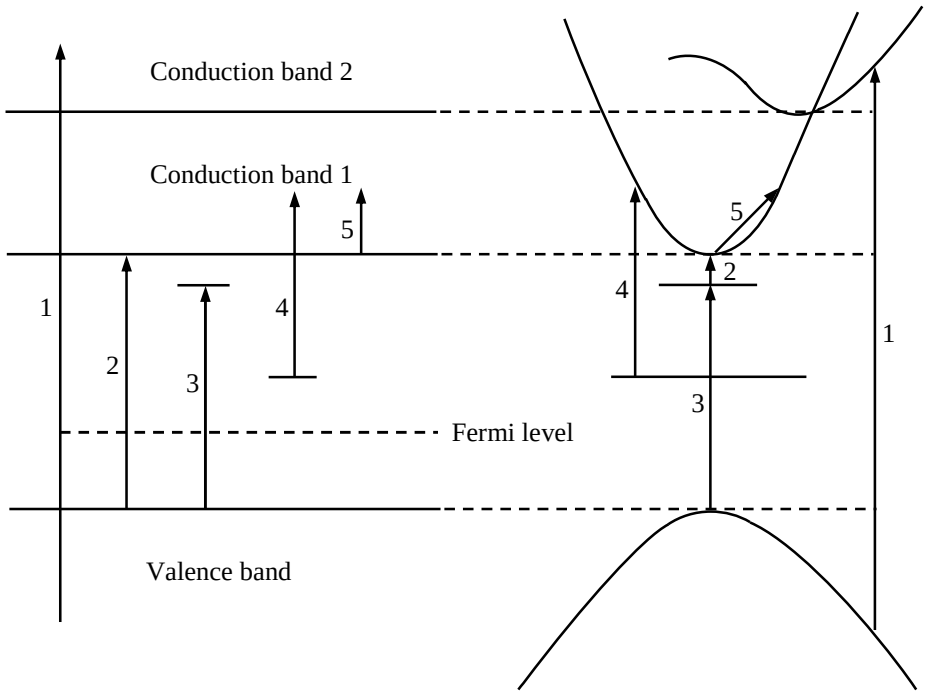

Figure 2.18 Characteristic types of optical transitions shown both for the flat - band model and for the *E* vs *k* plot. (1) Excitation from the valence band to higher - lying conduction bands, (2) excitation across the band gap, (3) exciton formation, (4) excitation from imperfections, (5) free - carrier excitation [78].

2.9 Electronic Configuration of Lanthanide Atoms in the Ground State [79]

The electronic configuration of an atom in the ground state is determined by its principal quantum number n and angular quantum number l. According to the principle of lowest energy, there are two types of electronic configurations for the lanthanide elements : [Xe] $4f^{\,n}\,6s^2$ and [Xe] $4f^{\,n-1}5d^{\,1}6s^2$. Here [Xe] represents the electronic configuration of xenon, which is $1s^22s^22p^63s^23p^63d^{\,10}4s^24p^64d^{\,10}5s^25p^6$, where n represents a number from 1 to 14. Lanthanum, cerium, and gadolinium belong to the [Xe] $4f^n6s^2$ type, while praseodymium, neodymium, promethium, samarium, europium, terbium, dysprosium, holmium, erbium, thulium, ytterbium, and lutetium belong to the [Xe] $4f^{\,n-1}5d^{\,1}6s^2$ type. Scandium and yttrium do not have $4f$ electrons but they do have similar chemical properties to lanthanide elements, because their outermost electrons have the $(n - 1)d^{\,1}ns^2$ configuration. For this reason, they are generally regarded as being lanthanide elements.

Lanthanide elements adopt either the [Xe] $4f^n6s^2$ or [Xe] $4f^{\,n-1}5d^{\,1}6s^2$ configuration depending on the relative energy level of these two electronic configurations. Figure 2.19 shows the

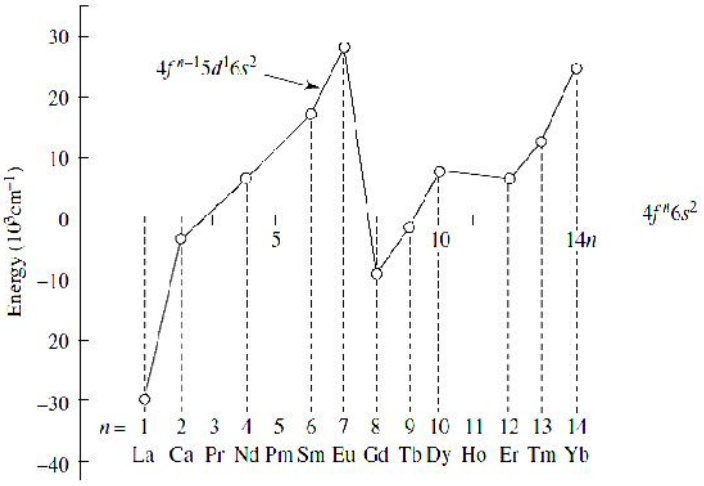

Figure 2.19 The relative energy level of the different electronic configurations, $4f^n6s^2$ or $4f^{n-1}5d^16s^2$ of neutral lanthanide atoms [80].

relative energy level of the neutral lanthanide atoms in the $4f^n6s^2$ or $4f^{n-1}5d^16s^2$ electronic configurations. For lanthanum, cerium, and gadolinium, the [Xe] $4f^{n-1}5d^16s^2$ configuration is lower in energy than the [Xe] $4f^n6s^2$ configuration, therefore, they adopt the former configuration. For terbium, two configurations [Xe] $4f^96s^2$ and [Xe] $4f^85d^16s^2$ are energetically close to each other so terbium can adopt either one. Lutetium has 14 4*f* electrons and therefore its only possible configuration is [Xe] $4f^{14}5d^16s^2$. The other elements all have a [Xe] $4f^n6s^2$ configuration. All the electronic configurations of lanthanide elements are summarized in Table 2.3.

Table 2.3 The electronic configurations of lanthanide elements.

		Electronic configurations of neutral atoms					Electronic configurations of trivalent ions	Atomic radius (pm) (coordination number =12)	Atomic weight
Z	Element	4*f*	5*s*	5*p*	5*d*	6*s*			
57	La	0	2	6	1	2	[Xe]$4f^0$	187.91	138.91
58	Ce	1	2	6	1	2	[Xe]$4f^1$	182.47	140.12
59	Pr	3	2	6		2	[Xe]$4f^2$	182.80	140.91
60	Nd	4	2	6		2	[Xe]$4f^3$	182.14	144.24
61	Pm	5	2	6		2	[Xe]$4f^4$	(181.0)	(147)
62	Sm	6	2	6		2	[Xe]$4f^5$	180.41	150.36
63	Eu	7	2	6		2	[Xe]$4f^6$	204.20	151.96
64	Gd	7	2	6	1	2	[Xe]$4f^7$	180.13	157.25
65	Tb	9	2	6		2	[Xe]$4f^8$	178.33	158.93
66	Dy	10	2	6		2	[Xe]$4f^9$	177.40	162.50
67	Ho	11	2	6		2	[Xe]$4f^{10}$	176.61	164.93
68	Er	12	2	6		2	[Xe]$4f^{11}$	175.66	167.26
69	Tm	13	2	6		2	[Xe]$4f^{12}$	174.62	168.93
70	Yb	14	2	6		2	[Xe]$4f^{13}$	193.92	173.04
71	Lu	14	2	6		2	[Xe]$4f^{14}$	173.49	174.97
		3*d*	4*s*	4*p*	4*d*	5*s*			
21	Sc	1	2				[Ar]	164.06	44.956
39	Y	10	2	6	1	2	[Kr]	180.12	88.906

2.10 Lanthanide Contraction [81]

For multi-electron atoms a decrease in atomic radius, brought about by an increase in nuclear charge, is partially offset by increasing electrostatic repulsion among the electrons. The shielding effect originates from the inner electrons and decreases according to : $s > p > d > f$. For lanthanide elements, as the atomic number increases an electron is not added to the outermost shell but rather to the inner 4*f* shell (Table 2.3). Because of their diffusive property, 4*f* electrons do not all distribute within the inner part of the 5*s*5*p* shell and this can be clearly seen in Figures 2.20 and 2.21. Figure 2.20 shows the radial distribution functions of 4*f*, 5*s*, 5*p*, 5*d*, 6*s* and 6*p* electrons for cerium and Figure 2.21 illustrates the radial distribution functions of 4*f*, 5*s*, 5*p* electrons for Pr^{3+}. An increase in 4*f* electrons only partly shields the increase in nuclear charge. It is generally believed that the screening constant of 4*f* electrons in trivalent lanthanide ions is about 0.85. The 4*f* electron clouds in neutral atoms are not as diffusive as in trivalent lanthanide ions and the screening constant of 4*f* electrons is larger but still less than one. Therefore, as the atomic number increases the effective attraction between the nucleus and the outer electrons increases. This increased attraction causes shrinkage in the atomic or ionic radius. This phenomenon is referred to as lanthanide contraction.

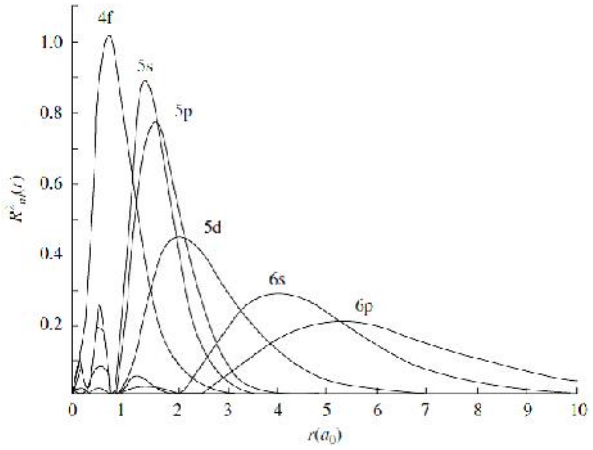

Figure 2.20 Radial distribution functions of 4*f*, 5*s*, 5*p*, 5*d*, 6*s* and 6*p* electrons for cerium [81].

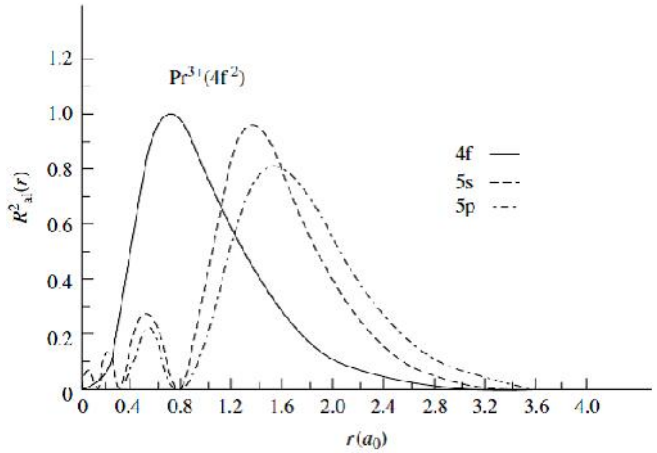

Figure 2.21 Radial distribution functions of 4*f*, 5*s*, 5*p* electrons for Pr^{3+} [82].

One effect of lanthanide contraction is that the radius of trivalent yttrium ion (Y^{3+}) is measured to be between that of Ho^{3+} and Er^{3+} and the atomic radius of yttrium is between neodymiumand samarium. This results in the chemical properties of yttriumbeing very similar to those of lanthanide elements. Yttriumis often found with lanthanide elements in naturalminerals. The chemical properties of yttriummay be similar to the lighter or the heavier lanthanide elements in different systems and this depends on the level of covalent character of the chemical bonds in those systems.

Another effect of lanthanide contraction is that the third rows of the d-block elements have only marginally larger atomic radii than the second transition series. For example, zirconium and hafnium, niobium and tantalum, or tungsten and molybdenum have similar ionic radii and chemical properties (Zr^{4+} 80 pm, Hf^{4+} 81 pm ; Nb^{5+} 70 pm, Ta^{5+} 73 pm ; Mo^{6+} 62 pm, W^{6+} 65 pm). These elements are also found in the same natural minerals and are difficult to separate.

Because of lanthanide contraction, the radius of lanthanide ions decreases gradually as the atomic number increases, resulting in regular changes in the properties of lanthanide elements as the atomic number increases. For example, the stability constant of lanthanide complexes usually increases as the atomic number increases ; the alkalinity of lanthanide ions decreases as the atomic number increases ; the pH at which hydrates start to precipitate from an aqueous solution decreases gradually as the atomic number increases.

Because of lanthanide contraction, the radius of lanthanide atoms also changes regularly. Because the shielding effect of 4*f* electrons in lanthanide atoms is not as strong as those in lanthanide ions, lanthanide contraction is weaker in lanthanide atoms than in ions. The atomic radius of a hexagonal crystal metal is defined as the average distance between adjacent atoms in a close–packed plane and in an adjacent close-packed plane (Table 2.3). The relationship between ionic radius and atomic number is shown in Figure 2.22. The atomic radius also exhibits lanthanide contraction, except for cerium, europium and ytterbium. However, the contraction of lanthanide atoms is not as prominent as that of lanthanide ions (Figure 2.23).

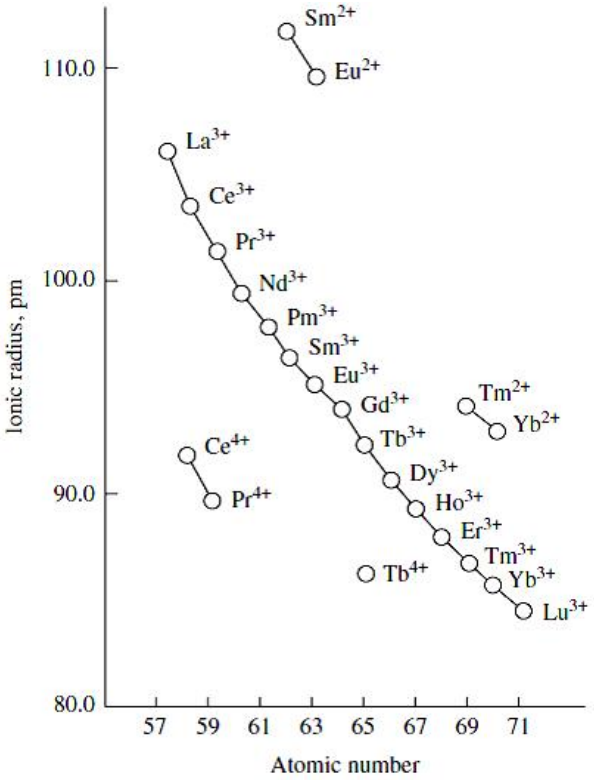

Figure 2.22 The relationship between ionic radius and atomic number of lanthanide ions [83].

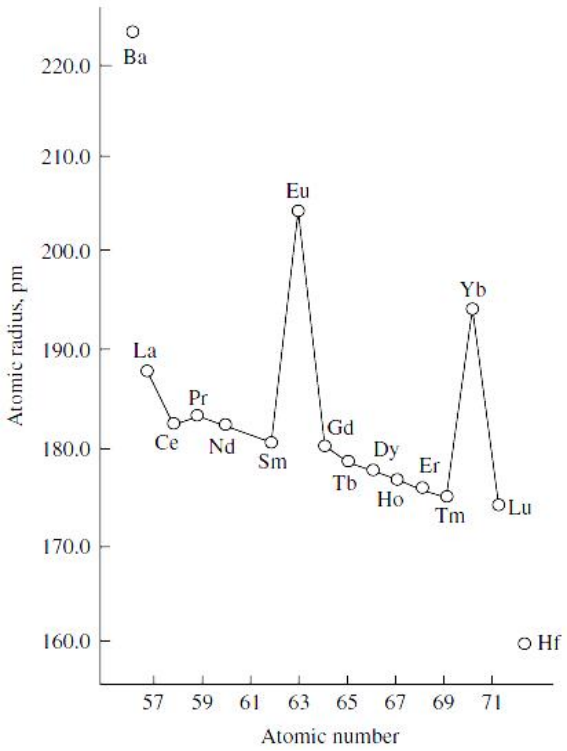

Figure 2.23 The relationship between atomic radius and atomic number of lanthanide atoms [83].

The abnormal behavior for the atomic radii of cerium, europium, and ytterbium can be explained as follows. The atomic radius of a metal approximately equals the radius of the maxima of the outermost electron cloud density. Therefore, the outermost electron clouds overlap in metals. These electrons can move freely in the crystal lattice and become conducting electrons. Generally speaking, there are three conducting electrons in lanthanide metals. Europium and ytterbium tend to maintain a $4f^7$ and $4f^{14}$ electron configuration, respectively, and thus they provide only two conducting electrons. The overlapping part of the outermost electrons between adjacent atoms becomes smaller and the atomic radius becomes larger. On the contrary, a cerium atom has only one 4*f* electron and it tends to provide four conducting electrons to obtain a stable electronic configuration. The overlapping part of the outermost electrons becomes larger, which causes the distance between adjacent atoms to become smaller compared with other lanthanide elements.

2.11 Specificity of the Photo Physical Properties of Rare Earth Compounds [79]

Because the 4*f* shells of lanthanide elements are unfilled, different arrangements of 4*f* electrons generate different energy levels. The 4*f* electron transitions, between the various energy levels, could generate numerous absorption and emission spectra.

Electronic configurations and spectral terms of ground state trivalent lanthanide ions are listed in Table 2.4. Figure 2.24 shows the energy level diagram for trivalent lanthanide ions.

Table 2.4 Electronic configurations and spectral terms of trivalent lanthanide ions in the ground state [84].

Ion	$4f^a$	Magnetic quantum number of 4*f* orbital							*L*	*S*	*J* *J=L–S*	Ground State spectral term
		3	2	1	0	–1	–2	–3				
La^{3+}	0								0	0	0	$^1S_0$
Ce^{3+}	1	↑							3	1/2	5/2	$^2F_{5/2}$
Pr^{3+}	2	↑	↑						5	1	4	$^3H_4$
Nd^{3+}	3	↑	↑	↑					6	3/2	9/2	$^4I_{9/2}$
Pm^{3+}	4	↑	↑	↑	↑				6	2	4	$^5I_4$
Sm^{3+}	5	↑	↑	↑	↑	↑			5	5/2	5/2	$^6H_{5/2}$
Eu^{3+}	6	↑	↑	↑	↑	↑	↑		3	3	0	$^7F_0$
Gd^{3+}	7	↑	↑	↑	↑	↑	↑	↑	0	7/2	7/2	$^8S_{7/2}$
Tb^{3+}	8	↑↓	↑	↑	↑	↑	↑	↑	3	3	6	$^7F_6$
Dy^{3+}	9	↑↓	↑↓	↑	↑	↑	↑	↑	5	5/2	15/2	$^6H_{15/2}$
Ho^{3+}	10	↑↓	↑↓	↑↓	↑	↑	↑	↑	6	2	8	$^5I_8$
Er^{3+}	11	↑↓	↑↓	↑↓	↑↓	↑	↑	↑	6	3/2	15/2	$^4I_{15/2}$
Tm^{3+}	12	↑↓	↑↓	↑↓	↑↓	↑↓	↑	↑	5	1	6	$^3H_6$
Yb^{3+}	13	↑↓	↑↓	↑↓	↑↓	↑↓	↑↓	↑	3	1/2	7/2	$^2F_{7/2}$
Lu^{3+}	14	↑↓	↑↓	↑↓	↑↓	↑↓	↑↓	↑↓	0	0	0	$^1S_0$

a the number of 4*f* electrons.

2.11.1 Spectral Terms [79]

There are four quantum numbers for describing the state of an electron, they are : principal quantum number *n*, which takes the value of 1, 2, 3, 4, . . . ; azimuthal quantum number, or orbital quantum number *l*, which takes the value of 0, 1, 2, 3, . . . , *n* - 1 ; the magnetic quantum number m_l, which takes the value of 0, ± 1, ± 2, ± 3 . . . ± l ; and the spin quantum 8 number *s*, which takes the value of ½ ; also, m_s is the spin magnetic quantum number. In addition, the electron in an atom has its spin movement, while also moving around the orbital. To describe this state, the overall angular quantum number, *j* was introduced. This is the vector sum momentum of *l* and *s*, that is, *j* = l + *s*, l + *s* - 1, . . . , |*l* - *s*|. m_j is the angular magnetic quantum number *j* along the magnetic field.

In a multi–electronic atom, the following quantum numbers can also be used to describe the energy levels, and the relationships between the quantum number of electrons are as follows.

1. Total spin quantum number $S = \sum m_s$.
2. Total orbital quantum number $L = m_l$.
3. Total magnetic orbital quantum number M_L.
4. Total angular momentum quantum number *J*, which takes $L + S$, $L + S - 1$, . . . $L - S$ when $L \geq S$, and can take $S + L$, $S + L - 1$, . . ., $S - L$ when $L \leq S$. M_J is the total magnetic angular quantum number *J* along the magnetic field.

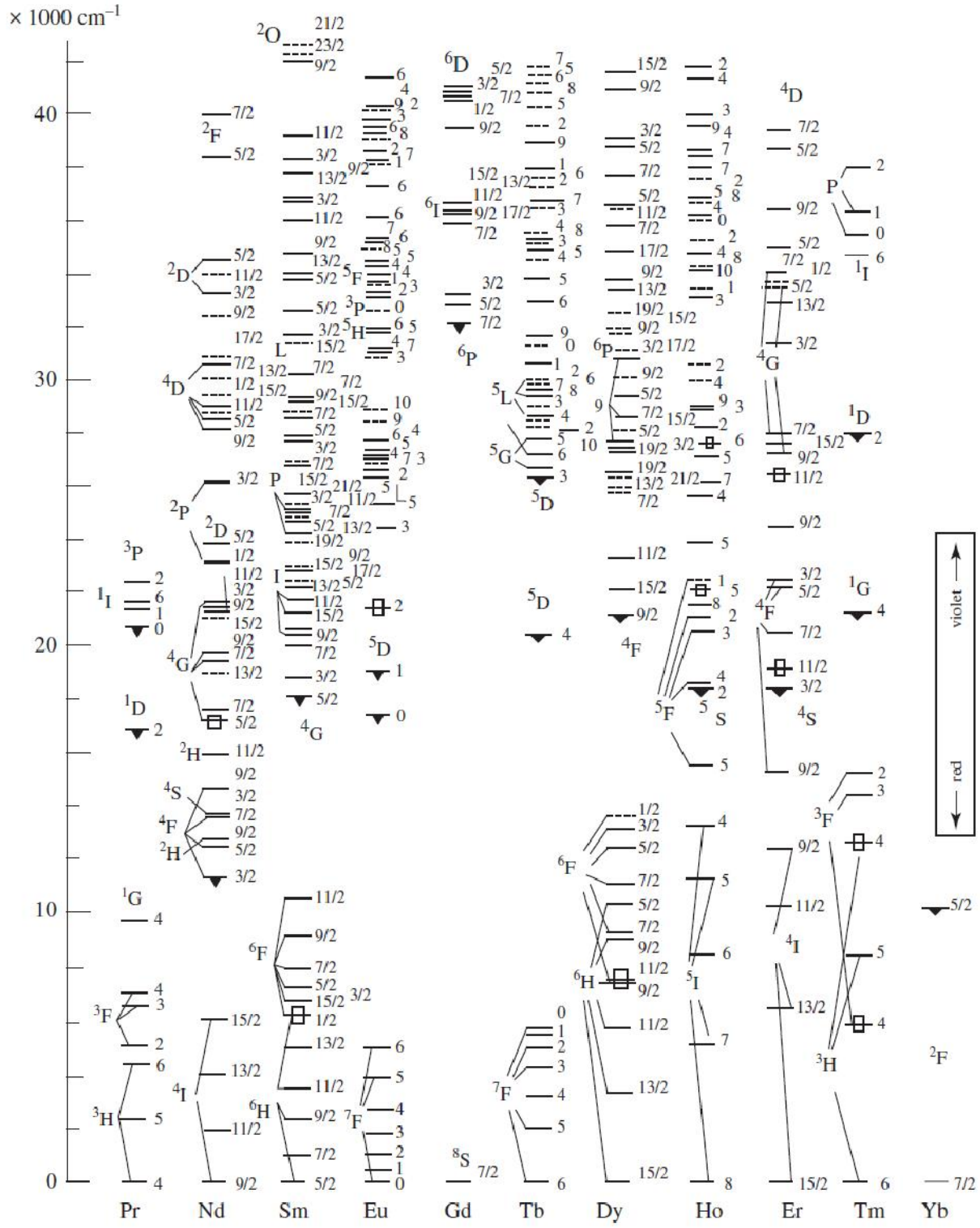

Figure 2.24 The energy level diagram for trivalent lanthanide ions [84].

The spectral term is a symbol which combines the azimuthal quantum number *l* and magnetic quantum number *m* to describe the energy level relationship between electronic configurations.

Seven orbital are present in the 4*f* shell (l = 3). Their magnetic quantum numbers are - 3, - 2, - 1, 0, 1, 2, and 3, respectively. When lanthanide elements are in their ground states the distribution of the 4*f* electrons in the orbital are as shown in Table 2.4.

In this table, M_L is the total magnetic quantum number of the ion. Its maximum is the total orbital angular quantum number L. M_s is the total spin quantum number along the magnetic field direction. Its maximum is the total spin quantum number S. $J = L \pm S$, is the total angular momentum quantum number of the ion and is the sum of the orbital and spin momentum. For the first seven ions (from La^{3+} to Eu^{3+}), $J = L - S$; for the last eight ions (from Gd^{3+} to Lu^{3+}), $J = L + S$. The spectral term consists of three quantum numbers, L, S, and J and may be expressed as $^{2S+1}L_J$. The value of L is indicated by S, P, D, F, G, H, and I for L = 0, 1, 2, 3, 4, 5, and 6, respectively. The number on the top left represents the multiplicity of the spectral term. It equals $2S + 1$. The number on the bottom right is the total angular momentum quantum number J. Take Nd^{3+} as an example, L = 6 and its corresponding capital letter is I ; S = 3/2 (three uncoupled electrons) so $2S + 1 = 4$; $J = L - S = 6 - 3/2 = 9/2$. Therefore, the spectral term for the ground state of Nd^{3+} is $^4I_{9/2}$.

2.11.2 Selection Rules for Atomic Spectra [79]

The 4*f* electrons of lanthanide elements can be placed in any 4*f* orbital except for La^{3+} (empty) and Lu^{3+} (full) and this result in various spectral terms and energy levels for lanthanide elements. For example, praseodymium has 41 energy levels at the $4f^3$, $6s^2$ configuration, 500 energy levels at the $4f^3$, $6s^1$, $6p^1$ configuration, 100 energy levels at the $4f^2$, $5d^1$, $6s^2$ configuration, 750 energy levels at the $4f^3$, $5d^1$, $6s^1$ configuration, and 1700 energy levels at the $4f^3$, $5d^2$ configurations. Gadolinium has 3106 energy levels at the $4f^7$, $5d^1$, $6s^2$ configuration while it's excited state $4f^7$, $5d^1$, $6s^1$, $6p^1$ has as many as 36000 energy levels. However, because of selection rule constraints many transitions between different energy levels are forbidden transitions and the number of visible spectral lines is far less than expected. Experimental data, which has subsequently been proved by quantum mechanical theory, shows that only transitions that satisfy the following rules are allowed :

1. For $L-S$ coupling (so called Russell–Saunders coupling), which is to combine the s of every electron to get S, and combine the l of every electron to obtain L initially and finally to combine S and L to get J :
   $\Delta S = 0$
   $\Delta L = \pm 1$
   $\Delta J = 0, \pm 1$, (except $0 \rightarrow 0$)
   $\Delta M_j = 0, \pm 1$ (for $\Delta J = 0$, except $0 \rightarrow 0$)

2. For j - j coupling, which is firstly to combine s and l for every electron to obtain j and then get the total angular quantum number J through j - j coupling :
   $\Delta j = 0, \pm 1$ (for the transition electron only), $\Delta j = 0$ (for the rest of the electrons)
   $\Delta J = 0, \pm 1$, (except $0 \rightarrow 0$)
   $\Delta M_j = 0, \pm 1$, (for $\Delta J = 0$, except $0 \rightarrow 0$)

In general, lanthanide atoms or ions with an unfilled 4*f* shell have about 30000 visible spectral lines. Transition metals with an unfilled 5*d* shell have about 7000 visible spectral lines. Main group elements with an unfilled p shell only have about 1000 visible spectral lines. Lanthanide elements, therefore, have more electronic energy

levels and spectral lines than the more common elements. They can absorb electromagnetic waves from the ultraviolet to the infrared and emit their characteristic spectra.

2.12 Luminescence [85]

Luminescence is originated by the radiative transitions between two states of atoms, molecules or extended molecular systems. A radiative transition is the one in which the energy is released in the form of photon. The nature of photon, the emission, depends on the nature of the initial and final state and the route to the excited state. The radiative luminescence takes place when the electronic transition takes place from the lowest excited state of singlet or triplet to the ground state. The radiative transition from singlet to ground state is a spin allowed transition and therefore the time scale of the transition is of the order of few nanoseconds. This type of radiative transition is known as fluorescence (Figure 2.25).
But the emission due to transition triplet to ground state is much larger, ranging from micro to several seconds because the process is spin forbidden. This transition from excited singlet to ground state passes via triplet state. This type of luminescence is called phosphorescence. So, luminescence can be divided into two kinds on the basis of emission.

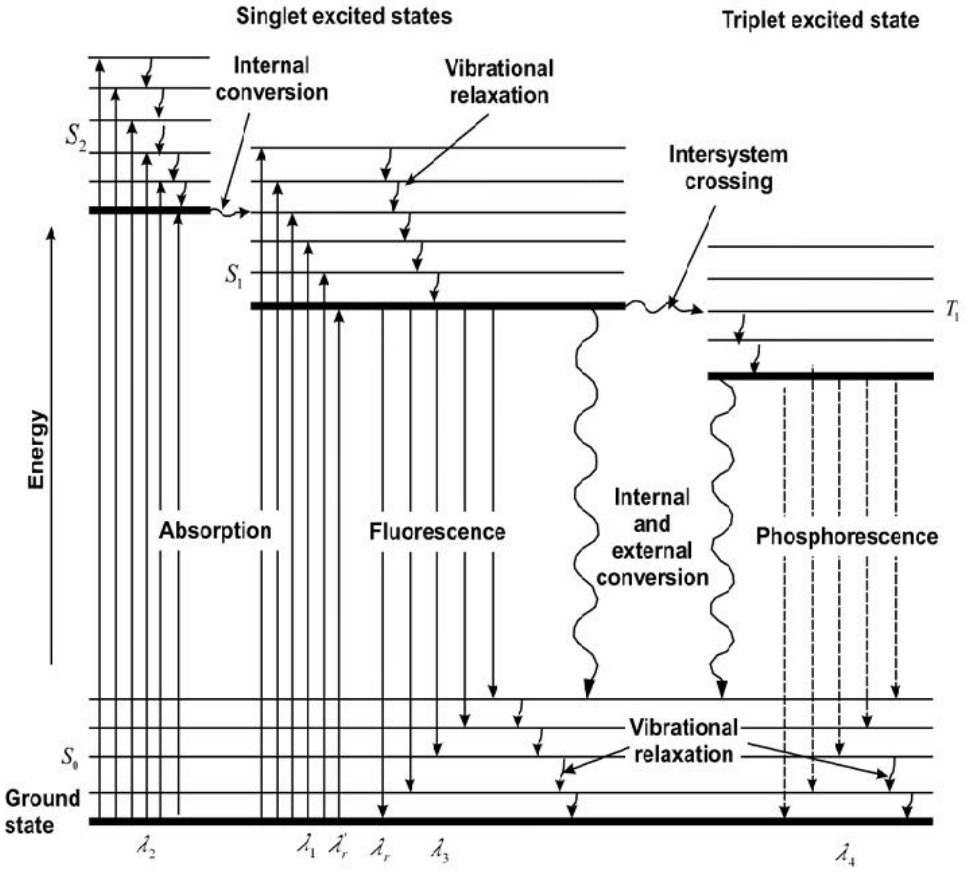

Figure 2.25 Various radiative and non-radiative processes in solid [90].

2.12.1 Fluorescence

Spin-allowed (ΔS = 0) transitions are called fluorescence. Fluorescence is a process in which a luminophore absorbs a suitable energy photon to raise an electron from an occupied orbital to a higher energy vacant orbital, followed by the electron returning back to the original ground state energy level and emitting a quantum of light with an energy corresponding to the energy difference between the excited state and ground state level, in such a way that the electron spin remains unchanged throughout the entire process. It means the molecule is either in its ground or excited singlet states all the time. This is a very fast process with luminescence lifetime of the order of nanoseconds. It quickly disappears when source of excitation (light or electric current) is removed.

2.12.2 Phosphorescence

Spin - forbidden transitions (ΔS = 1) are called phosphorescence. Phosphorescence is a type of luminescence that results from the delayed recombination of triplet excitons. Emission of light from the triplets is delayed because it is forbidden to occur in the same molecule by the Pauli Exclusion Principle. It may occur only when the triplet exciton exchange its energy or excited electron with another molecule what is known as intersystem crossing. The process of intersystem crossing usually takes significant time to occur. Phosphorescence usually complies with the Stokes rule, in which emitted light is shifted to the lower energy region (red-shifted). However, anti-Stokes phosphorescence exists that is also known as delayed fluorescence. It happens when two triplets recombine to form a neutral molecule and a singlet exciton that possess higher energy. The latter recombines to emit a photon of higher energy (blue-shifted). Luminescence lifetime of phosphorescence is micro to several seconds or longer. Internal conversion and other radiationless transfers of energy compete so successfully with phosphorescence that it is usually seen only at low temperatures or in highly viscous media.

2.13 Luminescence Process [86]

In order to understand luminescence process, we schematically depict our system, which comprises of a host lattice and a luminescent center (activator) showing excitation as well as radiative and non - radiative return to the ground state as shown in Figure 2.26.

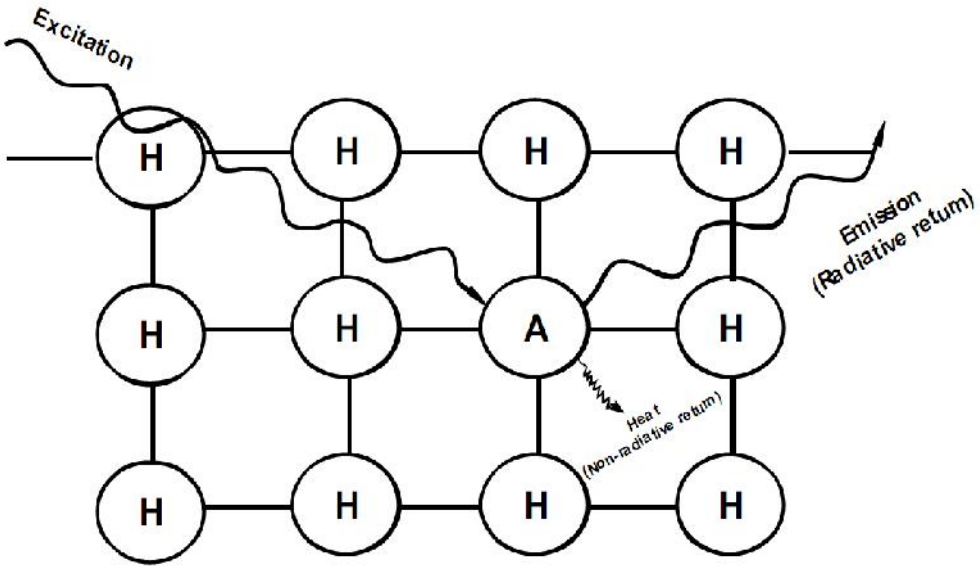

Figure 2.26 Luminescent ion A in its host lattice [90].

The exciting radiation is absorbed by the luminescent center, raising it to an excited state, which returns to the ground state by emission of radiation as drawn in Figure 2.27 producing luminescence.

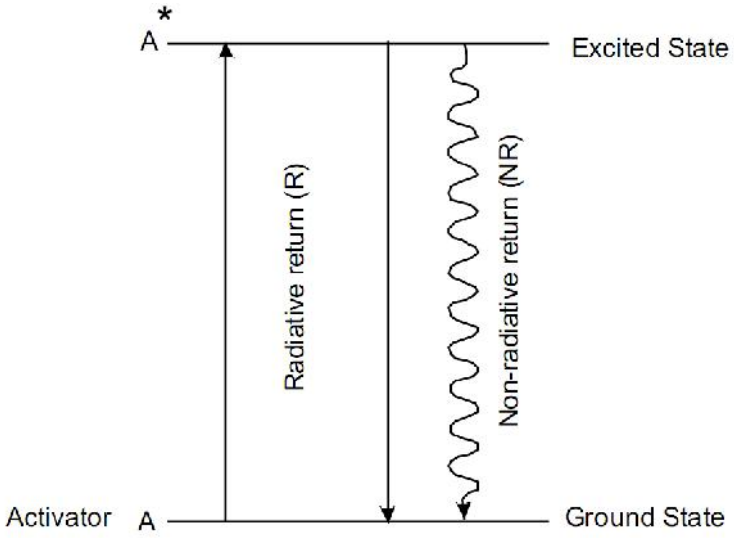

Figure 2.27 Schematic energy level scheme of the luminescent ion A [90].

Every ion and every material is not producing luminescence, to create luminescent materials, it is necessary to suppress the non - radiative process. As the non - radiative rates of return to the ground state determines the conversion efficiency of the luminescent material.

In 1867, Becquerel a famous scientist studied the luminescence in a red gemstone ruby (Al_2O_3:Cr^{3+}) using sunlight as the excitation source, but somehow his interpretation that luminescence, an intrinsic property, of the host lattice was not correct. In fact, in this gemstone the host lattice Al_2O_3 had no role other than to hold Cr^{3+} ion firmly and luminescent centre was the activator Cr^{3+} ion.

Some more complicated mechanisms occur in several luminescent materials, which involve ion other than activator in the host lattice. This ion called sensitizer, which absorbs the exciting radiation and transfers energy to the activator e.g. halophosphate phosphors. In some light emitting materials, energy transfer occurs within the sensitizer system which can be the host lattice. Energy transport by migration through the lattice occurs. e.g. ZnS: Ag^{+}, the blue emitting CRT phosphor. The ultra-violet radiation, electron beams and X - rays excite the S^{2-} host lattice which transfers this excitation energy rapidly to the Ag^{+} ions. The phenomenon is shown in Figure 2.28.

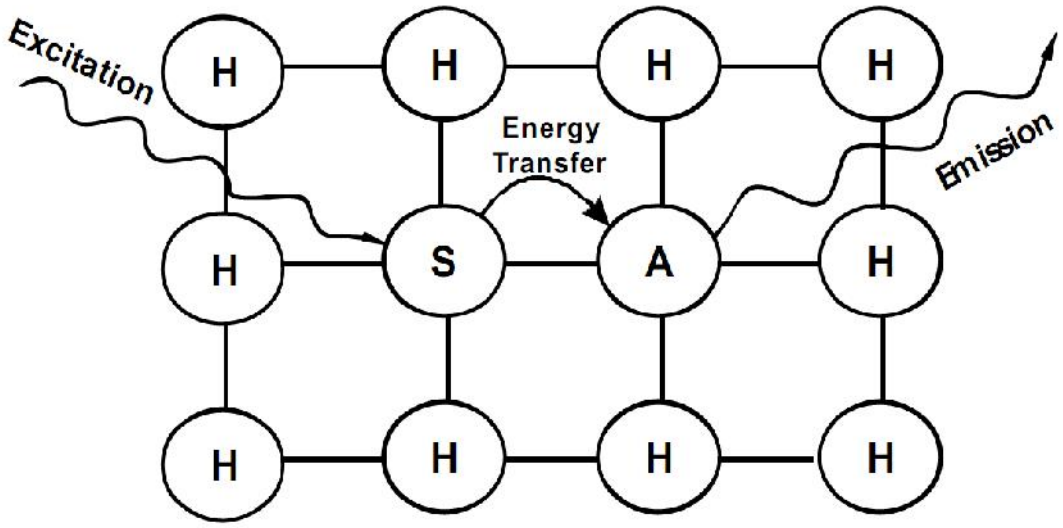

Figure 2.28 Luminescent material showing energy transfer from sensitizer S to an activator A [90].

There are some cases where the host lattice gets excited by the X-ray or electron beam e.g. $YVO_4:Eu^{3+}$. In this the host lattice VO_4^{3-} is excited by the ultra-violet radiations and this host lattice transfer its energy to Eu^{3+} ions, which emit red color.

The important physical processes which play a role in a luminescent material are described in detail as follows:

1. Excitation.
2. Emission.
3. Non-radiative return to the ground state.
4. Energy transfer.

1. Excitation

A luminescent material will only emit radiation when the excitation energy is absorbed. The material can be excited by ultraviolet or visible radiation, X - ray and γ - rays etc. The high - energy excitation by fast electrons / X - rays/ X - rays excites the host lattice, where as activator can be directly excited by ultra-violet/visible radiation.

The configurational co-ordinate diagram explains the shape of an optical absorption band. This diagram shows the potential energy curves of the absorbing centre as a function of configurational co - ordinate. This coordinate describes one of the vibrational modes of the centre involved. Let us consider a vibrational mode in which the central metal ion is at rest and the surrounding ligands are moving in phase away from the metal ion and coming back as shown in Figure 2.29. It is known as symmetrical stretching mode.

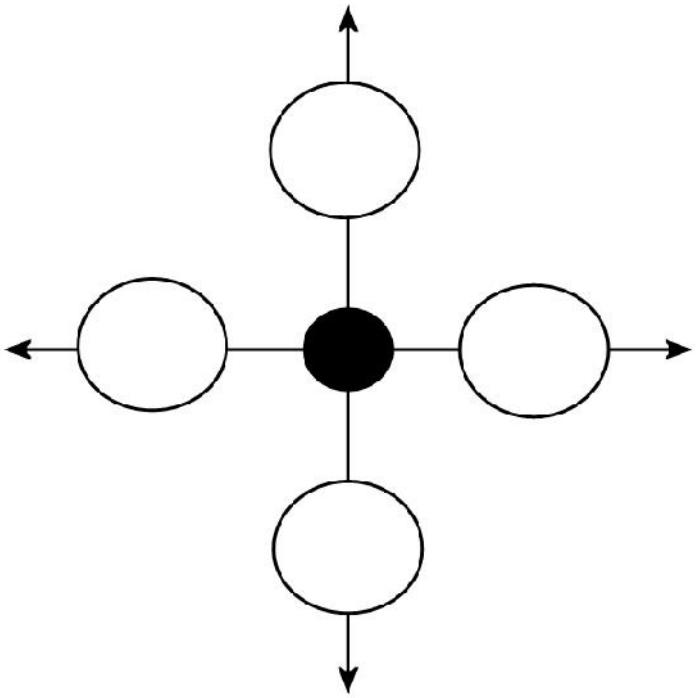

Figure 2.29 Symmetrical stretching vibration of a square-planar complex. The ligands (open circles) move in phase from and to the central metal ion [90].

The configurational coordinate diagram for this mode reduces to a plot of the energy E versus the metal ligand distance R, since R is the structural parameter, which varies during the vibration.

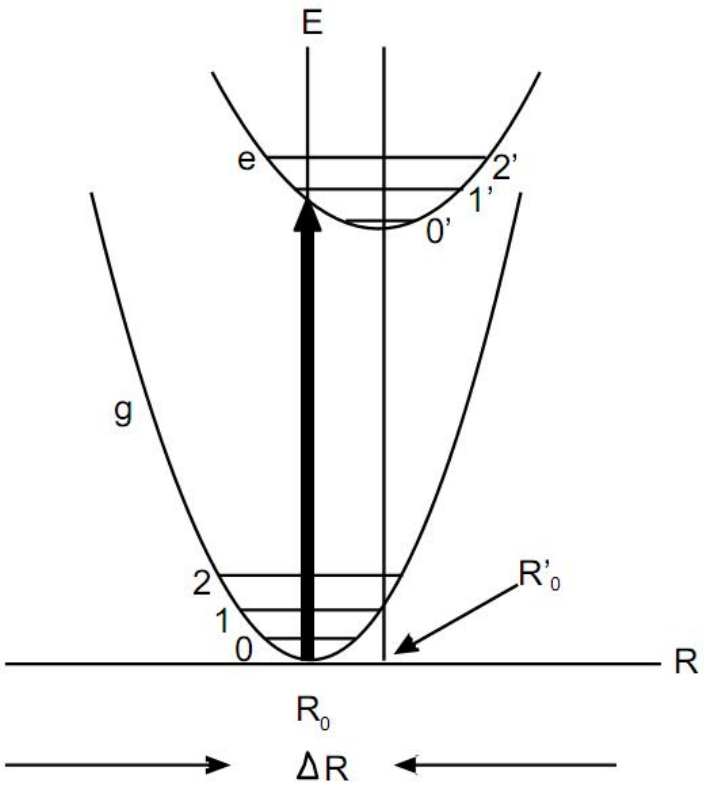

Figure 2.30 Configuration co-ordinate diagram. The ground state (g) has the equilibrium distance R_0; the vibrational states v = 0, 1, 2 are shown. The excited state (e) has the equilibrium distance R'_0; vibrational states v' = 0, 1, 2, are shown. The parabola offset is $\Delta R = (R'_0 - R_0)$ [90].

Figure 2.30 represents the configurational coordinate diagram where E is plotted versus R, the shape of ground state is parabolic as vibrational mode is assumed to be harmonic with a minimum at R_0. The restoring force F is proportional to the displacement:

$$F = -k\,(R - R_0) \tag{2.44}$$

and

$$E = \tfrac{1}{2}k\,(R - R_0)^2 \tag{2.45}$$

A force of this form corresponds to a potential energy and depends on R, which is parabolic and the minimum R_0 of the parabola is equal to the equilibrium distance in the ground state. The harmonic oscillator yields for the energy levels of the oscillator :

$$E_v = \left(v + \tfrac{1}{2}\right)h\nu \tag{2.46}$$

where

ν is the frequency of the oscillator and $v = 0, 1, 2, 3, \ldots$.
In the lowest vibrational level ($v = 0$) the highest probability of finding the system is at R_0, whereas for high value of v it is at the edges of the parabola. The wave functions of these vibrational levels are also known.

Similarly the excited states in the E - R diagram (Figure 2.30) are also represented by parabolas, but have different equilibrium distance (R'_0), force constant (k') and the parabolas are shifted by a value ΔR. These differences arise due to different chemical bonds in excited as well as ground state. The bonds are generally weaker in the ground state. This is shown in Figure 2.30, where the parabolas are shifted relative to each other over a value ΔR. The value $\Delta R = R'_0 - R_0$ is a qualitative measure of the interaction between the electrons and the vibrations of the optical centre under consideration.

In optical absorption the centre is promoted from its ground state to an excited state. These transitions are electronic, shown as vertical transition in co-ordinate diagram. The horizontal displacements in this diagram (Figure 2.30) are nuclear and distance R is the inter-nuclear distance. Since the electrons move much faster than the nuclei, the electronic transition takes, in good approximation, place in static surroundings. This implies a vertical transition as shown in Figure 2.30. The nuclei take their appropriate positions only later.

The optical absorption starts from the lowest vibrational level i.e. v = 0. Therefore the most probable transition occurs at R_0 where the vibrational wave function has its maximum value as represented in Figure 2.31.

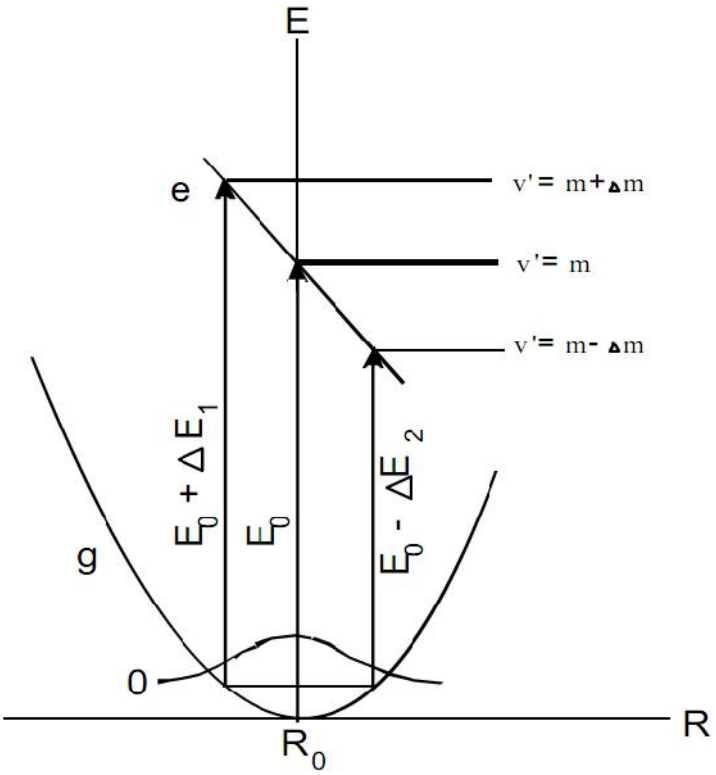

Figure 2.31 The optical absorption transition between two parabolas which have an offset relative to each other in the configurational co-ordinate diagram consists of a broad adsorption band [90].

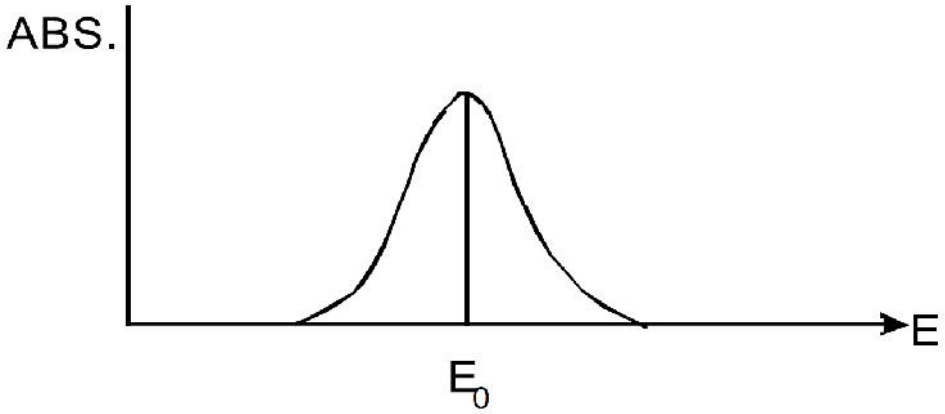

Figure 2.32 The optical absorption transition between two parabolas which have an offset relative to each other in the configurational co-ordinate diagram consists of a broad adsorption band continue [90].

The transition will end on the edge of the excited state parabola; since it is there that the vibrational levels of the excited state have their highest amplitude. This transition corresponds to the maximum of the absorption band. It is also possible although less probable, to start at R values larger or smaller than R_0. This leads to the width of the absorption band (Figure 2.32), because for R > R0 the energy difference of the transition will be less than for $R = R_0$ and for $R < R_0$ it will be larger. Two parabolas lie exactly above one another, if $\Delta R = 0$ and absorption band becomes a narrow line.

The probability for an optical transition between the v = 0 vibrational level of theground state and v = v' vibrational level of the excited state is proportional to :

$$(e/r/g)(\chi_{v'}/\chi_0) \qquad (2.47)$$

where

e: is the electronic wave function of the excited state.
g: is the electronic wave functions of the ground state.
r: is the electric-dipole operator driving the transition.
and χ : are the vibrational wave functions. To consider whole absorption band, one has to sum over v'.

This equation (2.47) consists of two parts :

(a) The electronic matrix element: this matrix element is independent of the vibrations and gives intensity of the transition.
(b) The vibrational overlap: this determines the shape of the absorption band.

The shapes of the absorption bands are understand as follows:

When $\Delta R = 0$, v = 0 and v' = 0 as the vibrational overlap is maximal for the levels.
The absorption spectrum consists of one line, due to the transition from v = 0 to v' = 0.
This transition is called the zero-vibrational or no phonon transition as no vibrations are involved. When $\Delta R \neq 0$, the v = 0 level will have the maximal vibrational overlap with several levels v' > 0, and results in a broad absorption band. The greater the ΔR value,

the broader is the absorption band. The width of an absorption band tells us about the magnitude of difference in chemical bonding between the ground state and excited state.

If $\Delta R = 0$; weak coupling case.
$\Delta R > 0$; intermediate coupling case.
$\Delta R >> 0$; strong coupling case.

Coupling here means the coupling between the electrons and vibrations of the centre. Only those transitions from ground state to excited state are possible which obey selection rules. Two important selection rules are as follows :

(i) The spin selection rules, which forbids electronic transition between levels with different spin states i.e. $\Delta S \neq 0$.

(ii) The parity selection rule which forbids electronic transition between levels with the same parity.

2. Emission

Emission from a luminescent centre is the radiative return to the ground state which can be explained on the basis of configurational co-ordinate diagram. Consider the configuration co - ordinate diagram Figure 2.33; assuming that there is an offset between the parabolas of the ground and excited state.

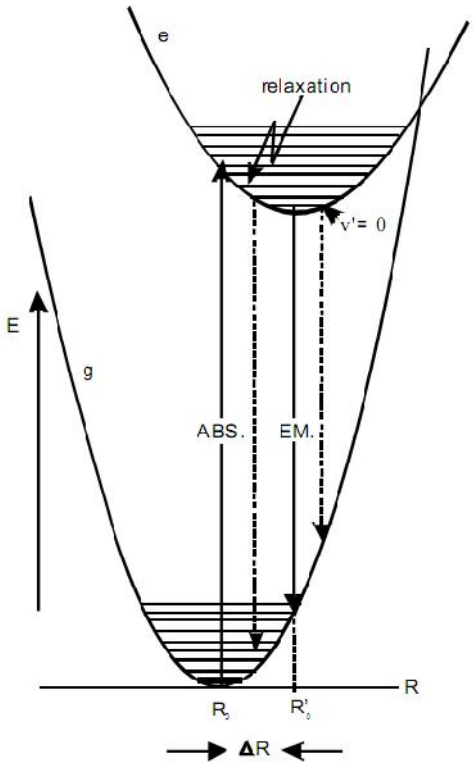

Figure 2.33 Configuration Co-ordinate Diagram [90].

The absorption process brings the luminescent centre in a high vibrational level of the excited state. The centre returns first to the lowest vibrational level of the excited state giving up the excess energy to the surroundings. Alternatively we can say that the nuclei adjust their positions according to the excited state, so that the inter-atomic distances equal the equilibrium distances belonging to the excited state. The configurational co-ordinate changes by ΔR. This process is called relaxation. During relaxation there occurs usually no emission and certainly not of high intensity. This can be easily seen from the rates involved: whereas a very fast emission has a rate 10^{8} s^{-1}, the vibrational rate is about 10^{-13} s^{-1}. Then from the lowest vibrational level of the excited state, the system can return to the ground state spontaneously emitting radiation. Rules for emission and absorption are same with a difference that emission occurs spontaneously but absorption occurs non-spontaneously. Absorption occurs only in presence of radiation field. The reverse process of absorption is stimulated emission.

As the center reaches a high vibration level of the ground state, by emission, relaxation process again occurs but now to the lowest vibrational level of the ground state and due to this relaxation process the emission occurs at a lower energy than absorption, all processes are shown in Figure 2.33.

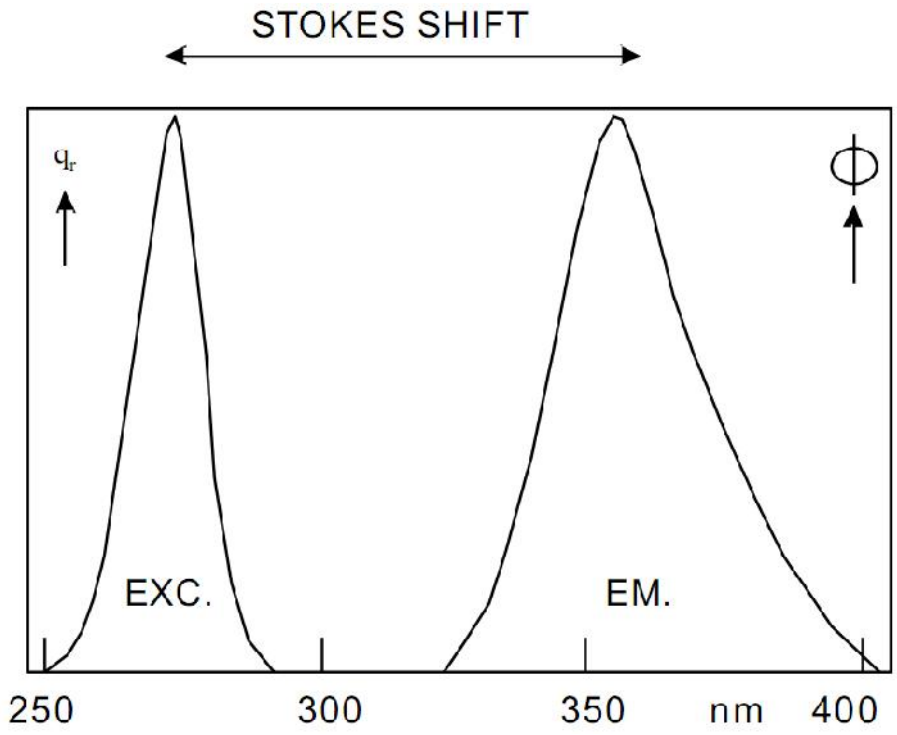

Figure 2.34 Emission and excitation spectra of the Bi^{3+} luminescence of LaOCl: Bi^{3+}. The Stokes shift amounts to about 9000cm^{-1}[90].

As an example, Figure 2.34 shows the emission and excitation (= absorption) spectra of luminescence of Bi^{3+} in LaOCl. The energy difference between the maximum of the excitation band and that of the emission band is called the Stokes shift. The greater the ΔR value the greater is the Stokes shift and broader the optical bands involved. In case if the two parabolas have equal force constants, they lose energy equal to S$h\nu$ per parabola in relaxation process where S being an integer and $h\nu$ is the spacing between two vibrational levels. The Stoke shifts results to 2S$h\nu$. S, is a constant and known as

Huang-Rhys coupling constant and measures the strength of the electron- lattice coupling.

$$S \alpha (\Delta R)^2 \quad (2.48)$$

If S < 1, it is weak coupling mode.
If 1 < S < 5, it is intermediate coupling mode.
If S > 5, It is strong coupling mode.

The life time for allowed emission transition is short of the order 10^{-7} - 10^{-8}s whereas strongly forbidden transition in solids it is much longer i.e. 10^{-3}s. This lifetime is of great importance in many applications and is discussed below. Assuming a two level system (Figure 2.34) i.e. excited state and ground state. The population of the excited state decreases according to :

$$\frac{dN_e}{dt} = -N_e P_{eg} \quad (2.49)$$

where

N_e= The number of luminescent ions in excited state after an excitation pulse
P_{eg}= Probability for spontaneous emission from the excited state to ground state
t = Time.

On integration, we get

$$N_e(t) = N_e(0)e^{-peg^1} \quad (2.50)$$

This can be rewritten as:

$$N_e(t) = N_e(0)e^{-\frac{1}{T_R}} \quad (2.51)$$

where

$$T_R = Peg^{-1}$$

It is called the radiative decay time. The plot of the logarithm of the luminescence intensity versus the time after the excitation pulse is a straight line i.e. in the agreement with equation (2.51).

3. Non-radiative transitions

A luminescent system on absorption of excitation energy can also return to the ground state without emission of radiation. This mode of returning to the ground state is known as non - radiative transition. This radiationless process always compete with the emission process, hence such processes must be suppressed to achieve highquantum efficiency of luminescent materials. To have a technical importance, a luminescent material should have high quantum efficiency which is the ratio of the number of quanta emitted to the number of quanta absorbed. Phosphors used in fluorescent lamps, usually have quantum efficiency of at least 0.75. All the quanta absorbed would be remitted if

there were no non - radiative losses. In order to study this relevant physical process by simple approximate method, let us consider the configurational diagrams (Figure 2.35).

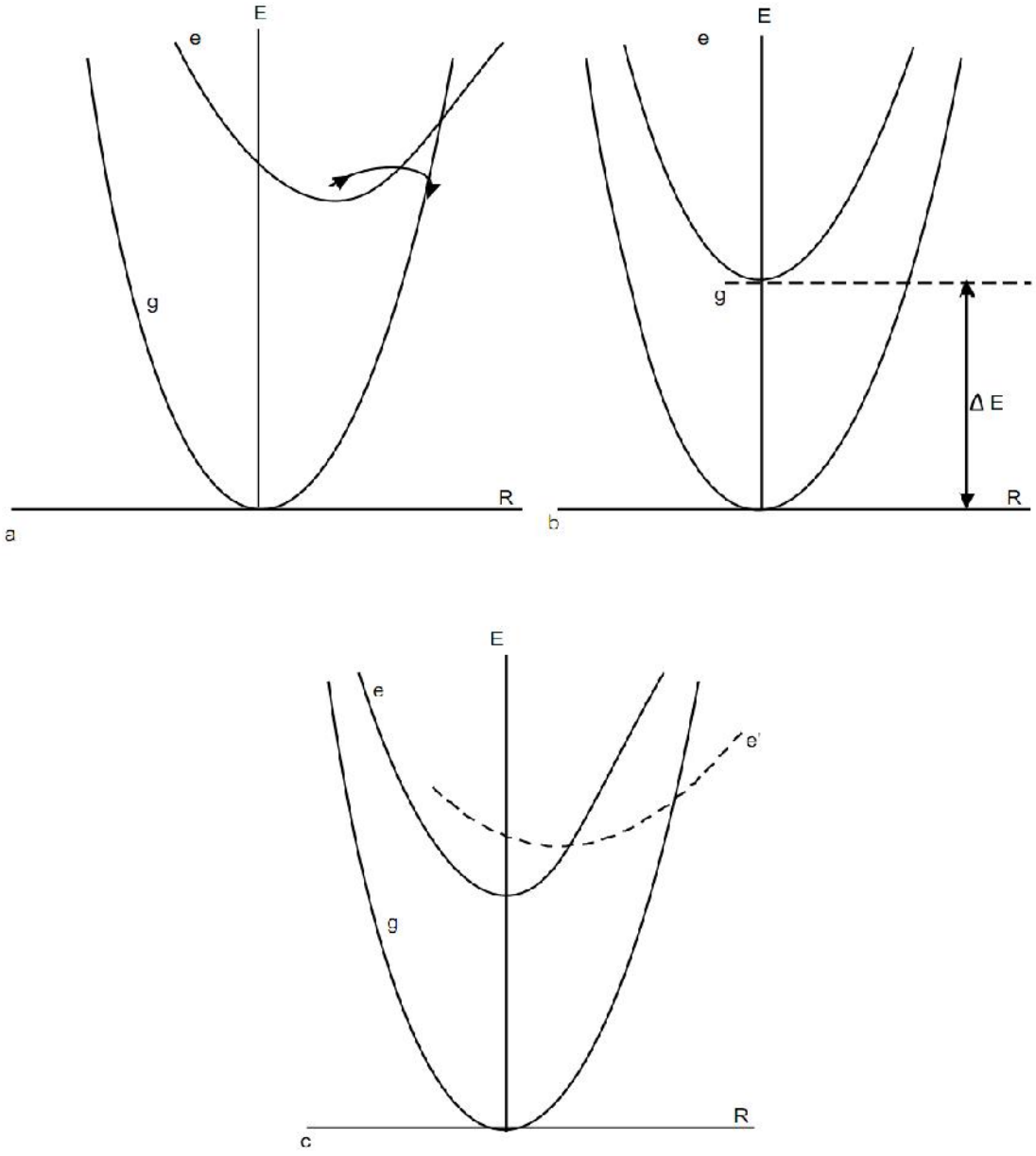

Figure 2.35 (a, b, c) Configurational co - ordinate diagrams showing non - radiative Transitions [90].

The possible absorption and emission transitions, stokes shifts relative to each other are shown in Figure 2.35 (a). At high temperature the relaxed - excited state may reach the crossing of the two parabolas. Through this crossing shown in Figure 2.35 (a) by an arrow, the non radiative transition may be possible to ground state, giving the excitation energy as heat to lattice. This model accounts for the thermal quenching of luminescence. The transition from parabola e to parabola g will not be considered further here. Essentially it is a transition between two resonant vibrational levels, one belonging to e and other to g. The transition occurs easily with larger offset between the parabolas.

If the parabolas are parallel (S = 0), they never cross each other Figure 2.35 (a). The non - radiative return to the state is possible if certain conditions are fulfilled i.e. the energy difference ΔE is equal to or less than 4 - 5 time the higher vibrational frequency of the surroundings. In that case, this amount of energy can simultaneously excite a few high - energy vibrations and is then lost for radiative process. This non radiative process is called multi-phonon emission.

The three parabolas-diagrams show both processes Figure 2.35 (c). The parallel parabolas will belong to the same configuration, so that they are connected by forbidden optical transitions only. The third one originates from a different configuration and is probably connected to the ground state by an allowed transition. This situation occurs often. Excitation occurs now from the ground state to the highest parabola in the allowed transition. From here the system relaxes to the relaxed excited state of the second parabola. Figure 2.35 (c) shows that the non radiative transition between the two upper parabolas is easy. Emission occurs now from the second parabola. This situation is found for $Al_2O_3:Cr^{3+}$. ($^4A_2 \rightarrow {}^4T_2$ excitation, $^4T_2 \rightarrow {}^2E$ relaxation, $^2E \rightarrow 4A_2$ emission), Eu^{3+} ($^7F \rightarrow$ charge - transfer state excitation, charge - transfer state to ^5D relaxation, $^5D \rightarrow {}^7F$ emission), and Tb^{3+} ($^7F \rightarrow 4f^7$ 5d excitation, $4f^7$ 5d $\rightarrow {}^5D$ relaxation, $^5D \rightarrow {}^7F$ emission).

The non - radiative processes are temperature dependent. The offset between the two parabolas (ΔR) is very important parameter for the non - radiative transition rate. This rate increases with increase in ΔR. The best understood non - radiative process are the weak coupling case (S ~ 0). The experimental data relate mainly to the rare earth ions, as far as their sharp line emission are considered i.e. intra $4f^n$ configuration transitions and find mention in various review papers.

4. Energy Transfer

In many luminescent materials, in addition to either emitting a photon or decaying non-radiatively to the ground state, an excited defect centre may also transfer energy to another centre either radiatively or non - radiatively. The ion that absorbs the exciting radiation and subsequently transfers it to the activator is called a sensitizer. This process is well explained by taking an example of $Ca_5(PO_4)_3F:Sb^{3+}$, Mn^{2+}. It is a well-known lamp phosphor having Sb^{3+} ion as sensitizer and Mn^{2+} as activator. The Sb^{3+} ion absorbs ultraviolet radiation from the mercury discharge and then transfers energy to Mn^{2+} as depicted in Figure 2.36, which is in its vicinity and emitted radiation, contain both blue (due to Sb^{3+}) and yellow (due to Mn^{2+}) emission.

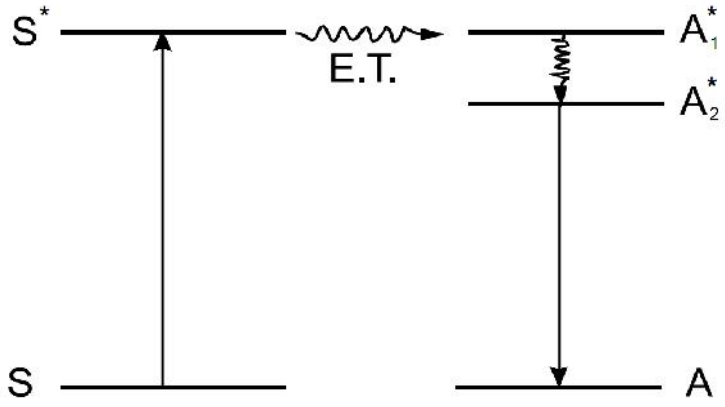

Figure 2.36 Energy transfer from a sensitizer to an activator [90].

Radiationless energy transfer is induced by an interaction between the state of system in which the sensitizer S is in its excited state and the activator A in the ground state, and the state in which the activator is excited and the sensitizer is in the ground state the probability per unit time for energy transfer is

$$P(S \rightarrow A) = \frac{(2\pi^2)}{h^2}\left|\int \varphi_S^e \varphi_A^g |V| \int \varphi_S^g \varphi_A^e \, dr\right|^2 \int f_{S^{em}} f_{A^{abs}} \, dv \qquad (2.52)$$

The frequency integral represents the overlap of the emission band of the sensitizer and the absorption band of the activator.

In the presence of energy transfer, the emission decay *I(t)* of a sensitizer ion is shortened :

$$I(t) = I(0)exp[-P(rod)t - P(S \rightarrow A)t] \qquad (2.53)$$

where *P*(rod) is the probability for decay in the absence of energy transfer. The measured luminescence decay is a statistical average of equation 9 over different sensitizer ions. The interaction V is usually expanded in terms of the distance between the sensitizer and activator ions giving rise to dipole-dipole (I/R^6), dipole - quadrupole (I/R^8) and quadrupole - quadrupole (I/R^{10}) contributions. The luminescence yield and decay of sensitizer emission in the presence of energy by each of the above mechanisms has been derived. An exchange interaction caused by the overlap of the wave functions on the sensitizer and activator ions that varies approximately as exp(- *c*R) can be lattice energy transfer. Because of the importance of radiationless energy transfer in many commonly used phosphors, energy transfer mechanisms have been studied extensively in the past.

If significant energy transfer occurs within the activators system, the excitation migrates through the lattice until it reaches sites in the lattice where the energy can be lost non-radiatively. This occurs in many phosphors once the activator concentration is increased above a critical concentration and is known as concentration quenching.
Finally, energy transfer through an excitation has been studied, at least theoretically. The exciting photon excites not a single defect center but a wave function that is a linear combination of the defect center wave functions.

2.14 Luminescence of Specific Rare-Earth Ions [87].

1. Eu^{3+} ($4f^6$)

The emission of Eu^{3+} ion is usually in the red spectral region and characteristics of $4f^6$ energy level transition emission. These emission lines correspond to the following transitions :

($^5D_0 \rightarrow {}^7F_4$, $^5D_0 \rightarrow {}^7F_3$, $^5D_0 \rightarrow {}^7F_2$, $^5D_0 \rightarrow {}^7F_1$ and $^5D_0 \rightarrow {}^7F_0$)

The spectra are dominated by the $^5D_0 \rightarrow {}^7F_2$ forced electric-dipole transition and the $^5D_0 \rightarrow {}^7F_1$ magnetic-dipole transition. The main emission peak is located at 605-625 nm, ascribable to the electric-dipole transition of $^5D_0 \rightarrow {}^7F_2$. This electric-dipole transition emission is utilized for practical application. The centre of strongest line is at 612nm.

2. Eu^{2+} ($4f^7$)

Eu^{2+} ion shows 5d→4f emission which can vary from long-wave length ultra- violet to yellow. The decay time is about 10^{-6} s. The ground state level of $4f^7$ is ^8S (octet) and the multiplicity of the emitting level is 6 or 8; the sextet portion of the emitting level contributes to the spin forbidden character of the transition. The f-f transition produce sharp line luminescence at ~360 nm and having a lifetime of milliseconds when the crystal field is weak so that the lowest excited state $4f^7$ (^6P_J) is lower than the $4f^6$ $5d^1$ state. The host crystals reported to produce ultra-violet luminescence are $SrAl_2O_4:Eu^{2+}$ [93], $SrAlF_5$ [94], $BaMg(SO_4)_2$ [95] and Sr(F,Cl) [96].

2.15 Lifetime [79].

The lifetime (τ) of an excited state is an important term when the kinetic process is of concern. The lifetime of an excited molecule is not a time measuring the existence of the excited state but is rather the deactivation time needed for excited states to reduce to 1/e of its initial population. It is defined as follows :

$$\tau = \frac{1}{\sum k_f} \tag{2.54}$$

where k_f is the rate constant of deactivation and $\sum k_f$ is the sum of all the rate constants of the deactivation processes, including radiative and non - radiative processes in the system.

Another characteristic of lanthanide elements is that some excited states have very long lifetimes ($10^{-2} \sim 10^{-6}$ s) while the average lifetimes of other typical atoms or ions range from 10^{-8} to 10^{-10} s. These long lifetime excited states are referred to as metastable states. These metastable states of lanthanide elements are caused by $4f \rightarrow 4f$ electronic transitions. According to the selection rules, these $\Delta l = 0$ electric dipole transitions are forbidden but are in fact observed. There are two major reasons for the forbidden transitions occurring: mixing between 4*f* configurations of opposite parity and the deviation of symmetry from an inversion center. Because lanthanide elements have many $4f \rightarrow 4f$ transitions between metastable states, the excited states of lanthanide elements have long lifetimes. This enables some lanthanide materials to be used in laser and fluorescence materials.

2.16 Absorption Spectra [79].

In lanthanide elements, the $5s^2$ and $5p^6$ shells are on the outside of the 4*f* shell. The $5s^2$ and $5p^6$ electrons are shielded, any force field (the crystal field or coordinating field in crystals or complexes) of the surrounding elements in complexes have little effect on the electrons in the 4*f* shell of the lanthanide elements. Therefore, the absorption spectra of lanthanide compounds are line–like spectra similar to those of free ions. This is different from the absorption spectra of d - block compounds. In d - block compounds, spectra originate from $3d \rightarrow 3d$ transitions. The *nd* shell is on the outside of the atoms so no shielding effect exists. Therefore, the 3d electrons are easily affected by crystal or coordinating fields. As a result, d–block elements show different absorption spectra in

different compounds. Because of a shift in the spectrum line in the d - block, absorption spectra change from line spectra in free ions to band spectra in compounds.

Most trivalent rare earth ions have no or very weak absorption in the visible range [97]. For example, Y^{3+}, La^{3+}, Gd^{3+}, Yb^{3+}, and Lu^{3+} in inorganic acid aqueous solutions are colorless. It is worth noting that colors of the aqueous solutions for ions having the 4*f*n electronic configuration are usually similar to those that have the $4f^{14-n}$ configuration (Figure 2.37).

Another characteristic of rare earth ions (except for Ce^{3+} and Yb^{3+}) in absorption spectra are their linear - like behavior. This comes from *f* - *f* transitions where 4*f* electrons exchange between different 4*f* energy levels. However, no *f* - *f* transition is allowed for Ce^{3+} ($4f^{1}$) or Yb^{3+} ($4f^{13}$). The broad absorption bands observed originates from configuration transitions, for example $4f^{n}$ to $4f^{n-1}5d^{1}$.

f - *f* transitions of lanthanide ions can be divided into magnetic dipole transitions and electric dipole transitions. In some cases an electric multi - dipole transition is also observed. According to the classic transition selection rule, a transition is forbidden when $\Delta L = 0$, that is, the *f* - *f* electric dipole transition is forbidden. However, it has been observed experimentally and this is because an odd parity term or an anti - parity electron is introduced into the $4f^{n}$ configuration to some extent.

The absorption spectra of rare earth complexes are mainly determined by the coordinated organic ligands.

Ce (colorless)
Pr (bright green)
Nd (rose red)
Pm (unknown)
Sm (light yellow)
Eu (near colorless)
Gd (colorless)
Tb (near colorless)
Dy (light yellow)
Ho (brown yellow)
Er (pink)
Tm (bright green)
Yb (colorless)

Figure 2.37 Similarity in color between ions with the electron configurations $4f^{n}$ and $4f^{14-n}$ [79].

2.17 The Emission Spectra of Rare Earth Compounds [79].

In the 1940s, emissions from rare earth complexes were observed and research into this phenomenon has received growing and lasting attention because of their potential application in optical communications, new generation displays and sensors.

Since the dipole strength of *f* - *f* transitions are formally forbidden, typically, these extinction coefficients are of the order of 1 $M^{-1}cm^{-1}$, an alternative path has to be used which is called luminescence sensitization or antenna effect, that is when the luminescent ion is coordinated with an organic ligand or imbedded into a matrix, then the energy absorbed will be transferred from the surrounding onto the luminescent ion and subsequently the ion emits characteristic light.

To quantitatively describe the effect of the emission, quantum yield *Q* is introduced, which has the following definition :

$$Q = \frac{\text{number of emitted photons}}{\text{number of absorbed photons}} \tag{2.55}$$

According to the emission properties, rare earth complexes can be divided into four groups as follows :

1. $Sm^{3+}(4f^5)$, $Eu^{3+}(4f^6)$, $Tb^{3+}(4f^8)$ and $Dy^{3+}(4f^9)$;
2. $Pr^{3+}(4f^2)$, $Nd^{3+}(4f^3)$, $Ho^{3+}(4f^{10})$, $Er^{3+}(4f^{11})$, $Tm^{3+}(4f^{12})$ and $Yb^{3+}(4f^{13})$;
3. $Sm^{2+}(4f^6)$, $Eu^{2+}(4f^7)$, $Yb^{2+}(4f^{14})$ and $Ce^{3+}(4f^1)$;
4. $Sc^{3+}(4f^0)$, $Y^{3+}(4f^0)$, $La^{3+}(4f^0)$, $Gd^{3+}(4f^7)$ and $Lu^{3+}(4f^{14})$.

For the first group, emissions originate because of the transition of 4*f* electrons from the lowest excited states to the ground states and the emissions are in the visible region. The probabilities of these transitions are relatively high and strong emissions may be observed. The lifetimes of these emissions are in the microsecond or milliseconds scale. For the second group, the energy levels of these ions are very close to one another. Thus, the emissions are often in the infrared region and their intensities are weaker than those of the first group by several orders of magnitude. All the ions in the third group exist in lower oxidation states and their emissions originate from *d* - *f* transitions and not *f* - *f* transitions, which would show broader emission bands. Obviously, the ions in the last group all have so - called stable electronic configurations, that is, their 4*f* orbital are either “empty’’, “half - filled’’ or “all - filled’’. Therefore, no *f* - *f* transitions occur except in gadolinium complexes, which emit in the ultraviolet region. However, these complexes do sometimes emit when suitable ligands are coordinated to the central ions. In these cases, the emissions are caused by ligand emission complexes.

2.18 X - ray Diffraction [88].

X - ray diffraction (XRD) is a quantitative analytical technique used for investigating nature of the material. Generally the solid matter can be divided as amorphous, crystalline materials. In amorphous materials (ex - Glasses) atom are arranged in a random way where as in crystals the atoms are arranged in a regular pattern, and there is as smallest volume element that by repetition in three dimensions describes the crystal. About 95% of all solid materials can be described as crystalline. When X - rays interact with substance, one gets a diffraction pattern. The X - ray diffraction pattern of a pure substance is, therefore, like a fingerprint of a substance. The powder diffraction method is thus ideally suited for characterization and identification of different phases in substance.

X - ray intensity versus scattering angle that is characteristic of atomic structure of the sample. The analysis is carried out with the help of Bragg's law. First of all W.L. Bragg showed that the X - rays reflected from a lattice plane and the effect associated with it could be derived by the equation as

$$n\lambda = 2d\sin\theta \text{ (Bragg's law)} \tag{2.56}$$

Here n = order of the spectrum or integer,
λ = The wavelength of X-rays,
d = The inter-planar spacing,
θ = The angle of incidence of X-ray beam on the lattice plane.

The equation (2.56) rewriting, then we get :

$$\sin\theta = \lambda/2d \tag{2.57}$$

Therefore the possible 2θ values where we can have reflections are determined by the unit cell dimension. However, the intensities of the reflections are determined by the distribution of the electrons in the unit cell. The highest electron density is found around atoms. Therefore, the intensities depend on what kind of atoms we have and where in the unit cell they are located. Planes going through areas with high electron density will reflect strongly, planes with low electron density will give weak intensities.

2.19 Fourier Transmission Infrared Spectroscopy [89-90].

The infrared region (10 - 14000 cm^{-1}) of the electromagnetic spectrum is divided into three regions: the near-, mid-, and far-IR. The mid-IR (400 - 4000 cm^{-1}) is the most commonly used region for analysis as all molecules possess characteristic absorbance frequencies and primary molecular vibrations in this range. Mid-infrared spectroscopy methods are based on studying the interaction of infrared radiation with samples. As IR radiation is passed through a sample, specific wavelengths are absorbed causing the chemical bonds in the material to undergo vibrations such as stretching, contracting, and bending. Functional groups present in a molecule tend to absorb IR radiation in the same wave number range regardless of other structures in the molecule, and spectral peaks are derived from the absorption of bond vibrational energy changes in the IR region. Thus there is a correlation between IR band positions and chemical structures in the molecule. In addition to providing qualitative information about functional groups, IR spectra can provide quantitative information, such as the concentration of bacteria in a growth medium.

An IR spectrum is measured by calculating the intensity of the IR radiation before and after it passes through a sample and the spectrum is traditionally plotted with Y-axis units as absorbance or transmittance and the X - axis as wave number units. For quantitative purposes it is necessary to plot the spectrum in absorbance units. FT - IR absorbance spectra follow Beer‘s law, which relates concentration to absorbance as in equation (2.58)

$$A_{\lambda} = L\varepsilon_{\lambda}c \tag{2.58}$$

where

A_{λ} = Absorbance,
L = Pathlength,
ε_{λ} = Absorptivity,
c = Concentration.

Transmittance is not directly proportional to the concentration and is defined in equation (2.59)

$$\%T = \frac{I_S}{I_R} \tag{2.59}$$

where

I_S = Intensity of IR beam after passing through the sample,
I_R = Intensity of IR beam before passing through the sample,
T = Transmittance

A general schematic of an FT - IR spectrometer is presented in Figure 2.38. The IR source emits radiation that is passed through an interferometer, usually a Michelson interferometer with a beam splitter (a semi - reflecting film usually made of KBr), a fixed mirror, and a moving mirror. The interferometer uses interference patterns to

make accurate measurements of the wavelength of light. When IR radiation is passed through a sample, some radiation is absorbed and the rest is transmitted to the detector. The detector measures the total interferogram from all the different IR wavelengths. A mathematical function called Fourier transform converts the interferogram (an intensity versus time spectrum) to an IR spectrum (an intensity versus frequency spectrum). Most mid - IR analyses are performed with a DTGS (deuterated triglycine sulfate) detector due to its ease of use and high sensitivity. When sample measurements must be made at high speed, the mercury cadmium telluride (MCT) detector is used which is 4 - 10 times more sensitive than the DTGS detector.

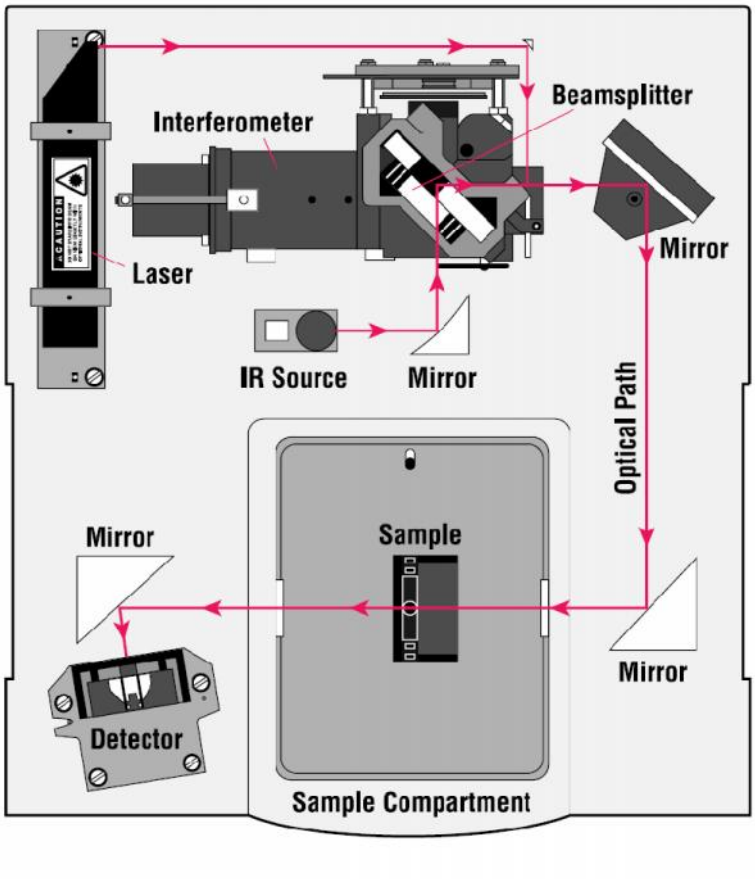

Figure 2.38 Basic Components of an FTIR System: The interferometer serves as the replacement counterpart for prisms (or diffraction gratings) used in traditional dispersion optics [93].

A background is used in order to remove all instrumental characteristics, thereby ensuring that the resulting spectrum is strictly a function of the sample only. The instrumentation process outlining the sequence of steps involved in using an FTIR is summarized in Figure 2.39.

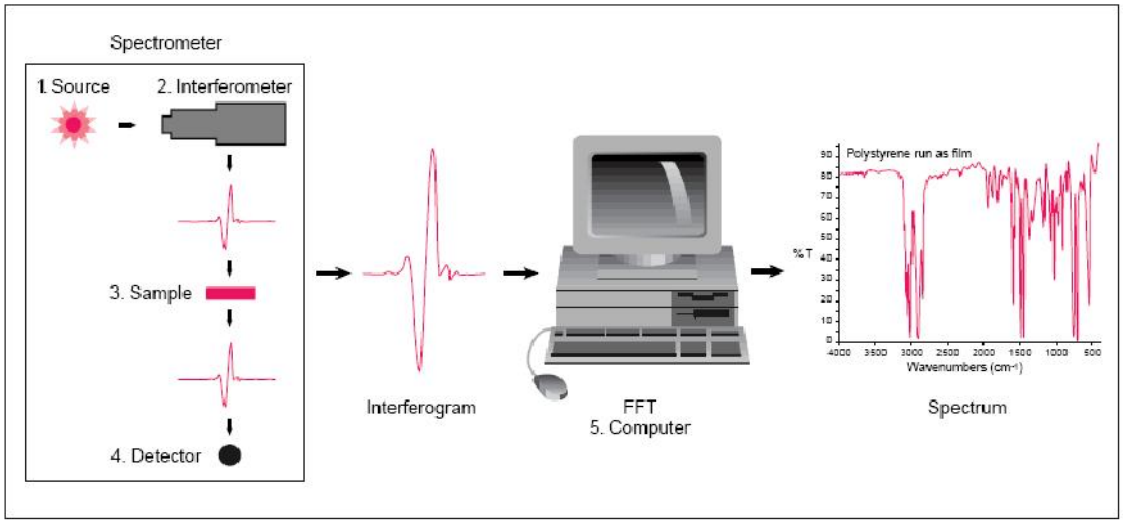

Figure 2.39 FTIR Instrumentation Process: The sequence of steps involved in obtaining an IR spectrum using an FTIR [93].